

FROM THE PLANAR ISING MODEL TO QUASICONFORMAL MAPPINGS

RÉMY MAHFOUF^A

ABSTRACT. We identify the scaling limit of full-plane Kadanoff–Ceva fermions on generic, non-degenerate s -embeddings. In this broad setting, the scaling limits are described in terms of solutions to conjugate Beltrami equations with prescribed singularities. For the underlying Ising model, this leads to the scaling limit of the energy–energy correlations and reveals a connection between the scaling limits of (near-)critical planar Ising models and quasiconformal mappings. For grids approximating bounded domains in the complex plane, we establish, in the scaling regime, the conformal covariance of the energy density on critical doubly periodic graphs. We complement this result with an analogous statement in the case where the limiting conformal structure generates a maximal surface (z, ϑ) in Minkowski space $\mathbb{R}^{(2,1)}$. All scaling factors obtained are local and expressed in terms of the geometry of the embedding, even in situations where they vary drastically from one region to another.

These results confirm the predictions of [12] and highlight that the scaling limits of generic (near-)critical Ising models naturally live on a substantially richer conformal structure than the classical Euclidean one.

1. INTRODUCTION

1.1. General context. What is the scaling limit of non-degenerate discrete harmonic functions on the complex plane, defined on a sequence of well-embedded planar graphs in the vanishing mesh limit? One might first naively expect that any limit is harmonic in the Euclidian metric. However, this turns out to be incorrect. In [57], Tutte introduced the notion of a barycentric embedding, aiming to provide an explicit procedure for drawing a 3-connected planar graph with straight-line edges. His method fixes the boundary of the graph as a non-intersecting convex polygon, while the interior vertices lie at the barycenter of their neighbors. It is possible to reverse engineer this construction and use Tutte barycentric embeddings to produce a discrete uniformization map for a finite abstract planar graph equipped with arbitrary conductances, giving some geometrical meaning to the underlying random walk. In a very recent work [46], it was shown that in full generality, any potential scaling limits of non-degenerate (Property **RW** in [46]) harmonic functions on Tutte embeddings can be expressed in terms of solutions to the linearized Monge–Ampère equation. In particular, the discrete embedding encodes a non-trivial conformal structure of the limit, which differs from standard harmonic analysis on the complex plane.

^A UNIVERSITÉ DE GENÈVE.
E-mail: `remy.mahfouf@unige.ch`.

The formalism of [46] belongs to a broader framework of *t-embeddings* or *Coulomb gauges* introduced in [36, 19, 18], which aims to study scaling limits of dimer models on general non-degenerate weighted planar graphs, beyond the integrable and symmetric case. A notable special example of *t-embeddings* is the notion of *s-embeddings* introduced by Chelkak [13, 12] for the Ising model. In the present article, one considers the planar Ising model with nearest-neighbor interactions and no external magnetic field, which has drawn considerable interest from both physics and mathematics over the last century (see the monographs [27, 44, 48] and references therein). We adopt conventions dual to the standard setup: spins of value ± 1 are assigned to the set G° of faces of a planar graph G . When G is finite and connected, each edge $e \in E(G)$, separating the faces $v_-^\circ(e)$ and $v_+^\circ(e)$, carries a positive coupling constant J_e . This defines a ferromagnetic model favoring configurations in which neighboring spins align. Given a positive inverse temperature $\beta > 0$, the corresponding probabilistic model assigns spins $\sigma \in \{\pm 1\}$ to G° , with partition function

$$\mathcal{Z}(G) := \sum_{\sigma: G^\circ \rightarrow \{\pm 1\}} \exp \left[\beta \sum_{e \in E(G)} J_e \sigma_{v_-^\circ(e)} \sigma_{v_+^\circ(e)} \right]. \quad (1.1)$$

An *s*-embedding provides a natural discrete conformal structure to a planar graphs equipped with Ising weights, similarly to a barycentric embedding for a planar graph equipped with random walk conductances. The embedding encodes both the combinatorics of the graph and the strengths of the coupling constants. For example, the square lattice with critical versus off-critical weights produces embeddings with drastically different large-scale geometries (see [12, Figure 2]). The construction is particularly well suited to generalizing the discrete analytic techniques introduced in Smirnov's seminal work on the critical square lattice [55, 54], which resolved the long-standing problem of conformal invariance for the critical nearest-neighbor Ising model on \mathbb{Z}^2 . Beyond Onsager's computation of the critical temperature on the homogeneous square lattice [47], exact identification of criticality had been obtained only for specific families of Ising weights: periodic lattices [21, 12, 26], Z-invariant weights on isoradial graphs [11, 50, 20], or their extensions via Lis' circle packings [38]. For generic collections of Ising weights, with no specific constraints on local graph structure or the value of the couplings, the work [40] proposed a general test for criticality of planar Ising models: starting from a combinatorial weighted graph (G, x) , one constructs a corresponding *s*-embedding and determines, through a concrete dichotomy on the embedding's discrete conformal structure, whether the model lies inside or outside a critical phase.

When studying scaling limits of (near-)critical Ising or dimer models on *s/t*-embeddings, a central theme of [19, 18] and [12, Section 2.7] is that all admissible scaling limits go far beyond the standard conformal co/invariance in the Euclidean metric (as predicted by Conformal Field Theory [7, 59]) or the massive Dirac equations that describe near-critical regimes [43, 53]. This is completely analogous to the appearance of linearized Monge-Ampère equations on barycentric embeddings. Beyond critical isoradial lattices and doubly-periodic graphs, where CFT predictions have been rigorously established, the appropriate general framework for describing all (near-)critical scaling limits involves quasiconformal mappings and solutions of conjugate Beltrami equations.

The purpose of this paper is to give the first concrete convergence results demonstrating these unexpected phenomena, which, to the best of our knowledge, have not yet been explored in the physics literature.

1.2. Definition of an s -embedding and the associated scale. To keep the presentation compact and self-contained, we postpone to Section 2 the detailed construction of an s -embedding \mathcal{S} , and begin with an informal overview of the tiling features obtained following the construction of [12]. Consider a weighted planar graph (G, x) with the combinatorics of the plane, defined up to homeomorphism preserving the cyclic ordering of edges. We denote its vertices by G^\bullet and its faces by G° , while the edges of the bipartite graph $\Lambda(G) := G^\bullet \cup G^\circ$ connect each vertex to the faces it belongs to. Each quad $z_e = (v_0^\bullet v_0^\circ v_1^\bullet v_1^\circ)$ of $\Lambda(G)$ can be identified with the edge e joining the vertices $v_{0,1}^\bullet$ and separating the faces $v_{0,1}^\circ$. Under this identification, one can construct a parametrization of the coupling constant $x(e)$ by the *abstract* angle

$$\theta_{z(e)} := 2 \arctan x(e) \in (0, \frac{\pi}{2}), \quad x(e) := \exp[-2\beta J_e]. \quad (1.2)$$

A proper s -embedding of (G, x) is a map $\mathcal{S} : \Lambda(G) \rightarrow \mathbb{C}$, such that

- The quad z_e is mapped to a quadrilateral $\mathcal{S}^\circ(z_e) = (\mathcal{S}(v_0^\bullet)\mathcal{S}(v_0^\circ)\mathcal{S}(v_1^\bullet)\mathcal{S}(v_1^\circ))$ which is tangential to a circle of radius r_{z_e} centred at a point $\mathcal{S}(z_e) \in \mathbb{C}$. The edge weight x_e can be recovered via the geometry of the tangential quadrilateral via the formulae (1.2) and (2.10).
- None of the tangential quadrilaterals degenerates to a segment while distinct faces do not overlap each other.

The guiding philosophy of the embedding construction is not to determine which weights are naturally associated with a given tiling of the plane by tangential quadrilaterals, but goes in the reverse direction. Given a prescribed set of weights, one looks for a discrete conformal structure on which local combinatorial relations for the associated Ising model naturally rewrite as discrete analytic questions. These embeddings are stable under rotations, translations, scalings, and complex conjugation.

Given a tiling \mathcal{S} of the plane made by tangential quadrilaterals, one can define on $\Lambda(G)$ the so-called origami map \mathcal{Q} , whose behavior acts as a test of criticality for the underlying Ising model. In short form (see Definition 2.2), the origami map is a real-valued function $\mathcal{Q} : \Lambda(G) \rightarrow \mathbb{R}$, defined up to an additive constant by its increments between neighboring vertices $\mathcal{S}(v^\bullet) \sim \mathcal{S}(v^\circ)$ by the local rule

$$\mathcal{Q}(\mathcal{S}(v^\bullet)) - \mathcal{Q}(\mathcal{S}(v^\circ)) := |\mathcal{S}(v^\bullet) - \mathcal{S}(v^\circ)|.$$

In words, \mathcal{Q} is defined on $G^\bullet \cup G^\circ$, adds edge lengths when going from vertices of $\mathcal{S}(G^\circ)$ to vertices of $\mathcal{S}(G^\bullet)$, and subtracts them in the opposite direction. Since the alternating sum of edge lengths in any tangential quadrilateral vanishes, this provides a consistent definition of \mathcal{Q} . To each edge $v^\bullet \sim v^\circ$ of $\Lambda(G)$, one can associate a *corner* $c = c(v^\bullet v^\circ)$ and an edge length δ_c in the \mathcal{S} -plane setting

$$\delta_c := |\mathcal{S}(v^\bullet) - \mathcal{S}(v^\circ)|.$$

Alternatively, one can view \mathcal{Q} as folding the tangential quadrilaterals along their diagonals (see, e.g., [19, Section 8.2]), which makes \mathcal{Q} a 1-Lipschitz function in the \mathcal{S} -plane.

Working on a general tiling made of tangential quadrilaterals- especially with locally very irregular grids-one should discuss a notion of *scale* before discussing any large scale property and limiting structure. This is not a priori trivial; we follow here the approach of [19], relying on the assumption $\text{LIP}(\kappa, \delta)$ stated below.

Assumption 1.1 ($\text{LIP}(\kappa, \delta)$). *We say that \mathcal{S} satisfies the assumption $\text{LIP}(\kappa, \delta)$ for some positive constants $\kappa < 1$ and $\delta > 0$ if, for any vertices $v, v' \in \Lambda(G)$,*

$$|\mathcal{S}(v') - \mathcal{S}(v)| \geq \delta \implies |\mathcal{Q}(v') - \mathcal{Q}(v)| \leq \kappa \cdot |\mathcal{S}(v') - \mathcal{S}(v)|. \quad (1.3)$$

In words, a grid \mathcal{S} satisfies $\text{LIP}(\kappa, \delta)$ if the origami map becomes a κ -Lipschitz function above the scale δ . Note that it was shown in [46, Section 5] that this notion of scale corresponds exactly to the distance at which the underlying random walks on the associated Tutte harmonic embeddings start behave like a diffusive process. The above assumption allows to define the notion of scale of the embedding \mathcal{S} relative to some given $\kappa < 1$.

Definition 1.1. We say that an s -embedding \mathcal{S} covering an open set $U \subseteq \mathbb{C}$ has a scale δ for the constant $\kappa < 1$ on U if

$$\delta = \delta^\kappa := \inf\{\hat{\delta} > 0, \text{LIP}(\kappa, \hat{\delta}) \text{ holds }\}. \quad (1.4)$$

In that case, we write $\mathcal{S} = \mathcal{S}^\delta = \mathcal{S}^{\delta^\kappa}$ (suppressing the explicit dependence on κ to lighten notation). Therefore, the scale of \mathcal{S} relative to a given κ is the smallest distance at which \mathcal{Q} becomes a κ -Lipschitz function. This article focuses on the scaling limit of Kadanoff–Ceva fermions along subsequences of s -embeddings $(\mathcal{S}^\delta)_{\delta > 0}$. In this framework, we always consider a sequence of s -embeddings $(\mathcal{S}^{\delta_n})_{\delta_n}$, where $\delta_n \rightarrow 0$ as $n \rightarrow \infty$, and each \mathcal{S}^{δ_n} satisfies $\text{Lip}(\kappa, \delta_n)$ for the same $\kappa < 1$. In particular, all $O(\cdot)$ constants appearing in this paper are uniform and depend only on $\kappa < 1$. Moreover, all constants of the form $C_i(\kappa)$ and $\gamma_i(\kappa)$ likewise depend solely on $\kappa < 1$ and may vary from one lemma, proposition, or theorem to another; nevertheless, each can, in principle, be expressed explicitly in terms of κ , following carefully the lines of [19, 12].

1.3. A criticality condition for a planar Ising model. When working on generic Ising models studied via their graphical representation in the s -embedding framework, the behavior of \mathcal{Q} encodes the model's criticality, at least in the sense of the strong box crossing property for the associated FK-Ising model (see [25, Chapters 4 and 5] for precise definitions and precise definitions of the Edwards–Sokal coupling). Still, the last sentence is slightly misleading, as the proofs made in this setup are based on discrete analysis techniques, and require some mild regularity on the structure of the embedding. Roughly speaking, on a grid of mesh size δ , the entire theory goes through provided there exists at least *one* skeleton of tangential quadrilaterals whose inner circle radius is larger than $\exp(-\delta^{-1})$. The requirement is formalized below, following [19, Assumption 1.2].

Assumption 1.2. *We say that a proper s -embedding \mathcal{S}^δ satisfies the assumption $\text{EXP-FAT}(\delta, \rho)$ on an open set U and for some $\rho > 0$ if*

after removing all quads $(\mathcal{S}^\delta)^\diamond(z)$ with $r_z \geq \delta \exp(-\rho \delta^{-1})$ from U , all vertex-connected components have diameter at most ρ .

In an s -embedding where both $\text{LIP}(\kappa, \delta)$ and $\text{EXP-FAT}(\delta, \rho)$ hold, the associated FK-Ising model satisfies the strong box crossing property starting at scales

comparable to ρ . More precisely, set

$$\square(\ell) := \left([-3\ell, 3\ell] \times [-3\ell, 3\ell]\right) \setminus \left((-3\ell, \ell) \times (-\ell, \ell)\right),$$

and fix a discretization $\square^\delta(\ell)$ of $\square(\ell)$ up to 10δ . Here by discretization we mean that the discrete boundary of $\square^\delta(\ell)$ is formed by edges of $\Lambda(\mathcal{S}^\delta)$, and the Hausdorff distance between the boundaries of $\square^\delta(\ell)$ and $\square(\ell)$, seen as discrete curves in the complex plane, is smaller than 10δ . In that setup, let $\mathbb{P}_{\square^\delta(\ell)}$ be the probability measure for the FK-Ising model with free boundary conditions on both boundaries of $\square^\delta(\ell)$. Then one has the following theorem, showing that starting at some scale, the Ising model behaves qualitatively like the critical square lattice, for which this statement was originally proven in [26].

Theorem 1.1 (Theorem 1.2 in [40]). *Fix an s -embedding \mathcal{S}^δ covering the disc $\mathbb{D}(0, 5\ell)$ and satisfying $\text{LIP}(\kappa, \delta)$ and $\text{EXP-FAT}(\delta, \rho)$. Then, there exists constants $L_0, p_0 > 0$, only depending on κ , such that for $\ell \geq L_0\rho$, one has*

$$\mathbb{P}_{\square^\delta(\ell)}[\text{there exists a wired circuit inside } \square^\delta(\ell)] \geq p_0.$$

A similar uniform estimate holds for the dual model.

We believe that the only conceptual assumption for Theorem 1.1 to hold is $\text{LIP}(\kappa, \delta)$, and the discussion in [40, Section 5.2] explains why this assumption on the origami map cannot be bypassed. As a consequence, on grids where both $\text{LIP}(\kappa, \delta)$ and $\text{EXP-FAT}(\delta, \rho)$ hold uniformly over the plane, there exists only one full-plane Gibbs measure, while the FK-interfaces are pre-compact. When studying scaling limits of the model, one should slightly weaken the $\text{EXP-FAT}(\delta, \rho)$ assumption, by requiring it to hold for a sequence of scales $\rho(\delta) \rightarrow 0$ as $\delta \rightarrow 0$.

Assumption 1.3. *We say that a sequence of proper s -embeddings $(\mathcal{S}^\delta)_{\delta > 0}$ satisfies $\text{EXP-FAT}_0(\delta, \rho(\delta))$ if, uniformly over the plane, there exists a function $\rho(\delta) \rightarrow 0$ such that each grid \mathcal{S}^δ satisfies $\text{EXP-FAT}(\delta, \rho(\delta))$ as $\delta \rightarrow 0$.*

The assumption $\text{EXP-FAT}_0(\delta, \rho(\delta))$ is required to hold uniformly over the entire complex plane to allow the analysis of infinite-volume Ising fermions. In terms of degeneracy, it allows, the existence of *small* connected components of tangential quadrilaterals whose inner circle is smaller than $\exp(-\rho(\delta)\delta^{-1})$, that must vanish in the limiting regime $\delta \rightarrow 0$. We believe that this condition still provides a flexible framework, which we hope could hold for embedding corresponding to random environments (see, e.g., [9, 29, 42]).

1.4. Main Results. In the present work, we study the scaling limit of full-plane Kadanoff-Ceva fermions, whose structure has only recently been postulated in [19, 18, 12] and appears to have no direct counterpart in the existing physics literature. We briefly recall the current state of the art on fermionic observables. It is by now well established that the scaling limit of the critical Ising model on the square lattice and on isoradial graphs is conformally invariant or covariant; see, for instance, [55, 54, 20, 15, 31, 16]. In this regime, limiting correlation functions and the laws of random interfaces in different planar domains are related by the conformal maps between these domains. In the near-critical case, correlations are instead governed by solutions of massive Dirac equations [50, 49, 17, 43, 1].

Within the general framework of s -embeddings, Chelkak observed in [12, Section 2.7] that the appropriate scaling limits should be described by solutions of *conjugate Beltrami equations* and, consequently, by quasiconformal mappings. When the limiting origami map $\mathcal{Q}^\delta \rightarrow \vartheta$ is smooth, this Beltrami formulation reduces to a massive Dirac equation, with a mass m admitting a purely geometric interpretation on the limiting surface $(\mathcal{S}^\delta, \mathcal{Q}^\delta)_{\delta>0} \subset \mathbb{R}^{2,1}$ embedded in Minkowski space (see [12, (2.29)], which emphasises the role of the $(2, 1)$ metric signature in distance computations). In particular, if the discrete surfaces $(\mathcal{S}^\delta, \mathcal{Q}^\delta)_{\delta>0}$ converge to a *maximal* surface in $\mathbb{R}^{2,1}$, that is, a surface $(z, \vartheta(z))$ with *vanishing mean curvature everywhere*, the underlying Ising model remains conformally invariant in the scaling limit, up to a change of variables to $\mathbb{R}^{2,1}$ encoded at the discrete level by the embedding. The convergence of interfaces in this setting was recently established in a beautiful work of Park [51]: interfaces *drawn at the discrete level* on $(\mathcal{S}^\delta, \mathcal{Q}^\delta) \subset \mathbb{R}^{2,1}$ converge to the standard SLE(16/3) *in the conformal parametrisation of the surface*.

By contrast, the analysis of correlation functions and the rigorous emergence of quasiconformal mappings-unavoidable when the limiting origami maps are no smoother than the automatic C^1 -has not previously been addressed in the Ising context, and no convergence results were available to confirm Chelkak's predictions. The present article fills this gap by relating discrete fermions on s -embeddings to solutions of quasiconformal mappings with prescribed singularities and asymptotic behavior at infinity. In the case of maximal surfaces, we further derive explicit formulae in both the full-plane and bounded-domain settings, in close analogy with the classical critical square-lattice and isoradial cases.

In all the theorems presented below, one works with a sequence of full-plane s -embeddings $(\mathcal{S}^\delta)_{\delta>0}$ that satisfy both $\text{EXP-FAT}_0(\delta, \rho(\delta))$ and $\text{LIP}(\kappa, \delta)$ for some $\kappa < 1$. As $(\mathcal{Q}^\delta)_{\delta>0}$ are κ -Lipschitz above scale $\rho(\delta)$ and defined up to additive constant, *one can always pass to a sub-sequence* and assume that $\mathcal{Q}^\delta \rightarrow \vartheta$ some κ -Lipschitz function, uniformly in compacts of \mathbb{C} . The following theorem represents the first generic and effective connection between the planar Ising model and quasiconformal mappings.

Theorem 1.2. *In the previous context, let c^δ and a^δ be two corners that respectively approximate c and a . Then as $\delta \rightarrow 0$ one has*

$$(\delta_{a^\delta} \delta_{c^\delta})^{-\frac{1}{2}} \langle \chi_{c^\delta} \chi_{a^\delta} \rangle_{\mathcal{S}^\delta} = \frac{1}{\pi} \text{Re} \left[\overline{\eta_{c^\delta}} F_\vartheta^{[\eta_{a^\delta}]}(c, a) \right] + o_{\delta \rightarrow 0}(1). \quad (1.5)$$

where the full-plane Kadanoff-Ceva fermion $\langle \chi_{c^\delta} \chi_{a^\delta} \rangle_{\mathcal{S}^\delta}$ is defined in Section 3.1, the complex signs $\overline{\eta_{c^\delta}}, \overline{\eta_{a^\delta}} \in \mathbb{T}$ are given by (2.7) and $F_\vartheta^{[\eta_{a^\delta}]}$ is defined at the end of Section 2.7. The error term $o_{\delta \rightarrow 0}(1)$ is uniform in $\kappa < 1$ and compacts of $\mathbb{C} \setminus \{c, a\}$.

Using the Pfaffian structure of Ising fermions, one can extend this theorem to the convergence of multi-point correlators, as stated in Theorem 4.1. More refined results can be derived through standard combinatorial techniques ([30, 58, 28, 14]), which strengthen the previous theorem in the case where the corners c^δ and a^δ are adjacent (that is, when the points c and a are fused). This makes it possible to identify the scaling limit of the energy density random variable $\varepsilon_e := \sigma_{e+} \sigma_{e-}$, which encodes the correlation between two neighbouring spins. After subtracting from ε_e its infinite-volume expectation and rescaling by the radius r_e of the associated tangential quadrilateral, the energy-energy correlations once again converge. The

scaling limit of this local correlation function is again described by solutions to the conjugate Beltrami equation. In what follows, fix $a_1 \neq a_2$ as distinct points in \mathbb{C} , respectively approximated by the edges e_1^δ and e_2^δ in \mathcal{S}^δ . This allows us to define the *normalized* energy random variables $\tilde{\varepsilon}_k := \varepsilon_{e_k} - \mathbb{E}_{\mathcal{S}^\delta}[\varepsilon_{e_k}]$. The relation between these energy correlations is expressed in the following theorem.

Theorem 1.3. *In the previous setup, one has as $\delta \rightarrow 0$*

$$\frac{\cos(\theta_{e_1^\delta}) \cdot \cos(\theta_{e_2^\delta})}{r_{e_1^\delta} \cdot r_{e_2^\delta}} \cdot \mathbb{E}_{\mathcal{S}^\delta}[\tilde{\varepsilon}_1 \cdot \tilde{\varepsilon}_2] = \frac{1}{\pi^2} (|F_\vartheta^*(a_1, a_2)|^2 - |F_\vartheta(a_1, a_2)|^2) + o_{\delta \rightarrow 0}(1), \quad (1.6)$$

where the functions F_ϑ^* , F_ϑ are constructed in Section 2.7, $o_{\delta \rightarrow 0}(1)$ is uniform in compacts of $\mathbb{C} \setminus \{a_1, a_2\}$ and $\kappa < 1$. If (z, ϑ) is maximal in $\mathbb{R}^{(2,1)}$, explicit formulae written in the conformal parametrisation (2.31) of the surface are given in (4.6).

Using once more the Pfaffian structure of Ising fermions, one can in principle extend the previous theorem to correlations involving n energy variables. In the previous theorems, all scaling factors are explicit and purely local. In particular, these results significantly extend the known statements for isoradial lattices, where a uniform scaling factor matches the global parameter δ that governs the entire grid. In the present setting, the scaling factors may vary substantially from place to place, yet still produce a well-defined scaling limit.

The present paper focuses on full-plane fermions, since in bounded regions the analysis of solutions to (Ising-type) Riemann-Hilbert boundary value problems introduced in [54] becomes difficult when holomorphicity of the gradients is replaced by conjugate Beltrami equations, and currently yields no explicit formulas. Sending the boundary to infinity bypasses this obstacle while still revealing the relevance of an unexpected conformal structure. Still, in bounded regions, it is possible to obtain explicit convergence statements and formulae in the specific case where conjugate Beltrami equations reduce to holomorphicity in a suitably chosen metric. The simplest new setting to address is that of critical doubly-periodic graphs, where conformal invariance is expected from universality principles but has been rigorously established only for FK interfaces; see [12, Theorem 1.2]. Our first contribution in bounded domains is to prove conformal covariance of the energy density observable in this setting for critical doubly-periodic graphs. This result goes beyond the isoradial framework and its strong integrability properties, previously treated by Hongler and Smirnov [31, 30]. Combined with [41], it completes the proof of universality of correlation functions for critical doubly-periodic graphs, extending well beyond the isoradial case. Fix a doubly-periodic s -embedding \mathcal{S} of the full plane, assuming that all its edges have length $\asymp 1$, and let $\mathcal{S}^\delta := \delta \cdot \mathcal{S}$ denote its rescaled version. For a simply connected domain Ω , let $\ell_\Omega(a)$ denote the hyperbolic metric element at a point $a \in \Omega$, defined by

$$\ell_\Omega(a) := 2|\psi'_a(a)|,$$

where $\psi_a : \Omega \rightarrow \mathbb{D}$ is a conformal map satisfying $\psi_a(a) = 0$. In the theorem below, we fix a smooth simply connected domain Ω discretized by $\Omega^\delta \subset \mathcal{S}^\delta$ in the Carathéodory sense, together with an interior point $a \in \Omega$ approximated by an edge e^δ adjacent to the quad z_{e^δ} . We denote by $\varepsilon_{e^\delta} = \sigma_{e_+^\delta} \sigma_{e_-^\delta}$ the energy density at e^δ . The universality of the energy density on critical doubly-periodic graphs can then be stated as follows.

Theorem 1.4. *In the previous periodic setup, one has as $\delta \rightarrow 0$*

$$\cos(\theta_{e^\delta}) \cdot \frac{\mathbb{E}_{\Omega^\delta}^{(w)}[\varepsilon_{e^\delta}] - \mathbb{E}_{\mathcal{S}^\delta}[\varepsilon_{e^\delta}]}{r_{e^\delta}} = \frac{\ell_\Omega(a)}{\pi} + o_{\delta \rightarrow 0}(1). \quad (1.7)$$

The techniques developed in [30] extend this result to multiple energy density observables on periodic graphs approximating bounded domains. The same arguments apply to s -embeddings with a *flat* origami map (see [12] for a precise definition), as well as to any setting, regardless of boundary regularity or discretization scheme, in which the limiting origami map satisfies $\vartheta \equiv 0$, provided that convergence of the FK martingale observables holds (see e.g. [39, Chapter 6] for a proof in smooth domains using techniques different from [51]). Note that in rough domains, one should combine an additional idea from [50, 58] to obtain the same conclusion.

Let us pass to explicit formulae on maximal surfaces. Consider a sequence $(\mathcal{S}^\delta)_{\delta > 0}$ of s -embeddings, each satisfying the assumption UNIF(δ) (that is, all geometric angles are bounded away from 0 and all edge lengths are comparable to δ). Passing to a subsequence, assume that $(\mathcal{S}^\delta, \mathcal{Q}^\delta)_{\delta > 0}$ converges to a *maximal surface* $(z, \vartheta(z)) \subset \mathbb{R}^{2,1}$ and that

$$|\mathcal{Q}^\delta(z) - \vartheta(z)| = O(\delta)$$

uniformly on compact subsets of the plane. Fix a smooth, bounded, simply connected domain $\Omega \subset \mathbb{C}$, a point $a \in \Omega$, and a quasiconformal parametrization $\zeta \mapsto z(\zeta)$ of the surface $(z, \vartheta(z))$ satisfying (2.31). Let a^* denote the preimage of a and Ω^* the preimage of Ω under this parametrization. Let $(\Omega^\delta)_{\delta > 0}$ approximate Ω in the Carathéodory sense, and let a be approximated by an edge e^δ adjacent to the quad z^δ . The following theorem shows, in that level of generality, conformal covariance of the energy density naturally arises on maximal surfaces in $\mathbb{R}^{2,1}$.

Theorem 1.5. *In the above setting, for the Ising model with wired boundary conditions, one has, as $\delta \rightarrow 0$,*

$$\cos(\theta_{e^\delta}) \frac{\mathbb{E}_{\Omega^\delta}^{(w)}[\varepsilon_{e^\delta}] - \mathbb{E}_{\mathcal{S}^\delta}[\varepsilon_{e^\delta}]}{r_{z_{e^\delta}}} = \frac{\ell_{\Omega^*}(a^*)}{\pi(|z_\zeta|(a^*) - |\bar{z}_\zeta(a^*)|)} + o_{\delta \rightarrow 0}(1), \quad (1.8)$$

where z_ζ and \bar{z}_ζ are the standard Wirtinger derivatives in the conformal parametrization (2.31) of the maximal surface $(z, \vartheta(z)) \subset \mathbb{R}^{(2,1)}$.

In particular, the discrete scaling factors remain the same as those of periodic or isoradial lattices, while the limiting objects are still conformally covariant, now taking into account the change of conformal structure induced by the embedding. This highlights that conformal covariance as formulated for isoradial or periodic lattices corresponds only to the special case in which the standard Euclidean plane is identified with the surface $\{x_3 = 0\}$ in Minkowski space $\mathbb{R}^{2,1}$.

1.5. Novelties of the paper, related works and open questions. The innovations of the present paper are both technical and conceptual, demonstrating the fundamental relevance of quasiconformal mappings and Lorentz geometry to the planar Ising model. From a technical standpoint, extending the convergence of correlation functions, even to doubly-periodic lattices, had long been obstructed by the absence of *discrete exponentials*, the central tool for identifying scaling limits and computing scaling factors on isoradial grids. All known proofs on isoradial grids rely crucially on this explicit family of solutions to (2.6) (see [35, 10, 11, 31,

[15, 17, 23]) to construct full-plane s -holomorphic functions with prescribed singularities, from which the scaling factors pop out. To overcome the lack of discrete exponentials, we introduce a more conceptual approach, previously unnoticed even for the critical square lattice, by identifying primitives of discrete fermions with Green functions. This integration-based perspective is reminiscent of the coupling-function analysis for dimers near their singularities [19, 18]. Note that, in contrast to the dimer setting, where no additional scaling is required, identifying Ising fermions necessitates determining nontrivial scaling factors whose nature remains obscure, especially on irregular grids. Representing the primitive of Ising fermions through a Green function not only heavily simplifies the analysis but also makes these scaling factors explicit, chosen to have an exact non-trivial discrete residue. Consequently, our results overcome the often needed finite-energy, bounded-angle, and edge-length comparability assumptions, allowing the computation of fermionic scaling limits even for highly degenerate local geometries with strong spatial discrepancies. In particular, the present results can be applied to previously known critical and massive setups considered via s -embeddings [20, 12, 38, 42].

Concerning the connection between the Ising model and quasiconformal mappings, we confirm Chelkak's prediction that conformal invariance and massive Dirac equations correspond only to particular instances within the full space of admissible conformal structures. Since *any spacelike surface can be approximated* by s -embeddings of the triangular lattice satisfying EXP-FAT($\delta, \rho(\delta)$) and LIP(κ, δ) (see e.g. [51, Remark 1.3] (see also the methods introduced in [2, 3])), our results imply that **every admissible conformal structure** in the sense of [12, Section 2.7] **arises from some planar Ising model**. Even conformal invariance in the Ising model is far richer than previously anticipated: these models naturally reside on maximal surfaces in $\mathbb{R}^{(2,1)}$. In particular, this Lorentzian geometric perspective generalizes Smirnov's original framework for conformal invariance beyond the Euclidean plane $\mathbb{R}^2 \subset \mathbb{R}^{(2,1)}$.

A major open question following this work concerns the scaling limit of general spin correlations. Unlike energy observables, such correlations cannot be directly expressed in terms of fermions, rendering their analysis substantially more difficult. The scaling factor $\delta^{1/8}$ per spin is known only from exact computations on isoradial grids (see, e.g., [44, 17]) and remains unpredictable beyond periodic settings. Establishing convergence for general spin correlations would therefore represent a significant advance.

Another natural direction is to extend the present results to bounded domains for general origami maps ϑ , by developing a theory of Riemann-Hilbert boundary value problems adapted to quasiconformal maps. Finally, full-plane fermions have further applications in embedding theory [42], where they appear as coefficients of a simple ODE/SDE governing the differential construction of a family of s -embeddings $(\mathcal{S}^{(t)})_{t \geq 0}$ of the graph $(G, x(t))_{t \geq 0}$ as the Ising weights $x(t)$ evolve continuously in time. We believe these results might contribute to a deeper understanding of conformal structures in Ising models in random environments, using the methods developed in [42].

Acknowledgements. I am first of all deeply indebted to Sung Chul Park with whom I started this project. Our discussions and some of his ideas were critical to this research. I am also indebted to Dmitry Chelkak for introducing me to this field and for the many enlightening discussions, as well as to Mikhail Basok for

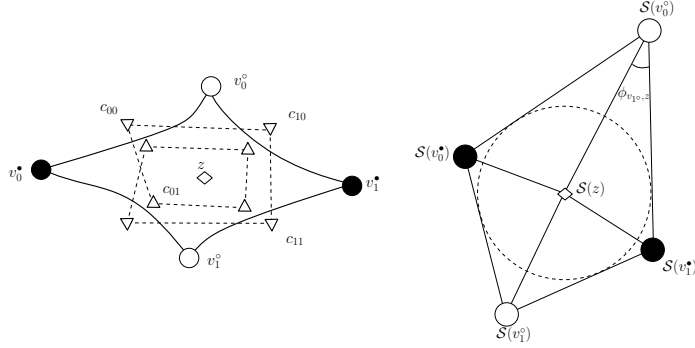


FIGURE 1. (Left) Notation around some given quad $z \in \diamond(G)$ with an arbitrary embedding in the plane. Vertices of the primal graph G^\bullet are represented as black dots while vertices of the dual graph G° , corresponding to faces of G , are represented as white dots. Moreover, the so called corners, which correspond to the edges of the bipartite graph $\Lambda(G) = G^\bullet \cup G^\circ$, are drawn as triangles. One represents in this picture a piece of the *double cover* of the corner graph branching around z . Corners that are neighbours *in that double-cover* are linked with dashed segments. (Right) A piece of one associated s -embedding containing the quad $S^\diamond(z)$, tangential to a circle of radius r_z centred at $S(z)$. The Ising weight of the edge attached to the vertices v_0^*, v_1^* can be recovered using the four angles $\phi_{v,z}$ attached to the quad $S^\diamond(z)$ using the formula (2.10).

his help on Beltrami equations. Finally I would like to thank Cédric Boutillier, Béatrice de Tilière, Dmitry Krachun, Benoit Laslier, Alexis Prevost, Yijun Wan, Sanjay Ramassamy and Yijun Wan for helpful discussions. This work was partially conducted during a visit to the Institute for Pure and Applied Mathematics (IPAM), which is supported by the National Science Foundation (Grant No. DMS-1925919). This research was funded by the Swiss National Science Foundation and the NCCR SwissMAP.

2. NOTATIONS AND BRIEF INTRODUCTION TO THE s -EMBEDDING FORMALISM

We recall in a concise and complete manner the general construction of s -embeddings introduced in [12, Section 3], together with the regularity theory of s -holomorphic functions, both based on a complexification of the standard Kadanoff–Ceva formalism. We also recall the link between s -embeddings and their dimer counterpart, the so-called t -embedding framework [19, 36], which is crucial for our specific problem. The notation follows exactly that of [12, 40] and agrees with [14, Section 3], [13], and [19, 18]. We do not provide any proofs below and refer the reader to [12, Section 2] for more details. Chelkak’s original idea was to construct a class of embeddings associated with a given weighted abstract graph, where the weights have a geometric interpretation, making discrete complex analysis techniques applicable.

2.1. Notation and Kadanoff–Ceva formalism. Let us fix G a planar graph (allowing the presence of multi-edges and vertices of degree 2 but not allowing loops and vertices of degree one) with the combinatorics of the plane or the sphere. The graph G should be understood up to homeomorphisms preserving the cyclic order of edges around each given vertex. In the sphere case, one also prescribes one of the faces of G and calls it the outer face. One denotes by $G = G^\bullet$ the original graph whose vertices are represented by $v^\bullet \in G^\bullet$ and G° its dual, whose vertices are represented by $v^\circ \in G^\circ$ and correspond to the faces of G . The faces of the graph $\Lambda(G) := G^\circ \cup G^\bullet$ (with natural incidence relation in a bipartite graph) are in straightforward bijection with edges of the graph G . One also denotes $\diamond(G)$ the graph dual to $\Lambda(G)$, corresponding to its faces, and whose vertices are listed by $z \in \diamond(G)$. One calls this graph the quad graph. Finally, one denotes by $\Upsilon(G)$ the medial graph of $\Lambda(G)$. The vertices of $\Upsilon(G)$, which are called corners of G , are in direct bijection with edges $(v^\bullet v^\circ)$ of $\Lambda(G)$. To make the Kadanoff–Ceva formalism fully consistent, one needs to work in general with several double covers of the graph $\Upsilon(G)$, see e.g. [45, Fig. 27] or [12, Fig 3.A] for relevant pictures of those double-covers. In the current paper, one denotes by $\Upsilon^\times(G)$ the double cover that branches over *all* the faces of $\Upsilon(G)$, meaning around each element of the type $v^\bullet \in G^\bullet, v^\circ \in G^\circ, z \in \diamond(G)$. When G is a finite graph, this definition remains meaningful as $\#(G^\bullet) + \#(G^\circ) + \#(\diamond(G))$ is an even number. Fixing $\varpi = \{v_1^\bullet, \dots, v_m^\bullet, v_1^\circ, \dots, v_n^\circ\} \subset \Lambda(G)$, where the integers n, m are both even, one denotes by $\Upsilon_\varpi^\times(G)$ the double cover of $\Upsilon(G)$ branching over all its faces *except* those ϖ , together with $\Upsilon_\varpi(G)$, the double cover of $\Upsilon(G)$ which branches *only* over the faces of ϖ . A function defined on one of the aforementioned double covers and whose value at two different lifts of the same corner differ only by the sign (meaning here a multiplicative factor -1) is called a *spinor*.

In this paper, one works with the Ising model on faces of graph G , including the outer face in the disc case, meaning that one imposes *wired* boundary conditions. This statistical mechanics model produces a random assignment of ± 1 variables to vertices of G° , following the partition function (1.1). The associated low-temperature expansion [14, Section 1.2] maps a spin configuration $\sigma : G^\circ \rightarrow \{\pm 1\}$ to a subset C of edges of G separating spins of opposite sign. Such mapping is 2-to-1, depending on the value taken by the spin attached to the outer face.

One can fix an even number n of vertices $v_1^\circ, \dots, v_n^\circ \in G^\circ$ and a subgraph $\gamma^\circ = \gamma_{[v_1^\circ, \dots, v_n^\circ]} \subset G^\circ$ with odd degree only at vertices of $v_1^\circ, \dots, v_n^\circ$ and even degree at all the other vertices of G° . Such a configuration can be viewed as a collection of paths on G° linking in a pairwise fashion the vertices of $v_1^\circ, \dots, v_n^\circ$. Denoting

$$x_{[v_1^\circ, \dots, v_n^\circ]}(e) := (-1)^{e \cdot \gamma_{[v_1^\circ, \dots, v_n^\circ]}} x(e), \quad e \in E(G),$$

where $e \cdot \gamma = 0$ if the edge e doesn't cross the path γ and $e \cdot \gamma = 1$ otherwise, we obtain the correlation formula

$$\mathbb{E}[\sigma_{v_1^\circ} \dots \sigma_{v_n^\circ}] = x_{[v_1^\circ, \dots, v_n^\circ]}(\mathcal{E}(G)) / x(\mathcal{E}(G)), \quad (2.1)$$

where $x(C) := \prod_{e \in C} x(e)$, $x(\mathcal{E}(G)) := \sum_{C \in \mathcal{E}(G)} x(C)$, and similarly for $x_{[v_1^\circ, \dots, v_n^\circ]}$.

If once again m is even and $v_1^\bullet, \dots, v_m^\bullet \in G^\bullet$, one can fix a subgraph $\gamma^\bullet = \gamma_{[v_1^\bullet, \dots, v_m^\bullet]} \subset G^\bullet$ with an even degree at all the vertices of G^\bullet except those belonging to $v_1^\bullet, \dots, v_m^\bullet$. In the spirit of the formalism of Kadanoff and Ceva [32], one can change the signs of the interaction constants $J_e \mapsto -J_e$ on edges $e \in \gamma^\bullet$, which is

equivalent to replacing $x(e)$ by $x(e)^{-1}$ along the edges of γ^\bullet and making the model anti-ferromagnetic near γ^\bullet . This amounts to consider the random variable (which as for now still depends on the choice of γ^\bullet)

$$\mu_{v_1^\bullet} \dots \mu_{v_m^\bullet} := \exp \left[-2\beta \sum_{e \in \gamma^{[v_1^\bullet, \dots, v_m^\bullet]}} J_e \sigma_{v_-^\circ(e)} \sigma_{v_+^\circ(e)} \right].$$

Using the domain walls representation one can see that (e.g. [14, Proposition 1.3])

$$\mathbb{E}[\mu_{v_1^\bullet} \dots \mu_{v_m^\bullet}] = x(\mathcal{E}^{[v_1^\bullet, \dots, v_m^\bullet]}(G)) / x(\mathcal{E}(G)), \quad (2.2)$$

where $\mathcal{E}^{[v_1^\bullet, \dots, v_m^\bullet]}$ is the set of subgraphs with an even degree everywhere except at vertices of $v_1^\bullet, \dots, v_m^\bullet$, which have odd degrees. Passing to expectation in (2.2), the result doesn't now depend on γ^\bullet anymore. The relevant observation is that one can generalize (2.1) and (2.2) to the presence of spins and disorder at the same time, which reads this time as (e.g. [14, Proposition 3.3])

$$\mathbb{E}[\mu_{v_1^\bullet} \dots \mu_{v_m^\bullet} \sigma_{v_1^\circ} \dots \sigma_{v_n^\circ}] = x_{[v_1^\circ, \dots, v_n^\circ]}(\mathcal{E}^{[v_1^\bullet, \dots, v_m^\bullet]}(G)) / x(\mathcal{E}(G)), \quad (2.3)$$

where the variable $\mu_{v_1^\bullet} \dots \mu_{v_m^\bullet}$ keeps the same definition as above. Still, an additional difficulty appears for those mixed correlations. Indeed, this time, the sign of the last expression actually depends on the parity of the number of intersections between the paths γ° and γ^\bullet . There isn't a canonical way to fix that sign in (2.3) staying on the Cartesian product structure $(G^\bullet)^{\times m} \times (G^\circ)^{\times n}$. To bypass this difficulty, one can fix $\mathcal{S} : \Lambda(G) \rightarrow \mathbb{C}$ an arbitrarily chosen embedding of G , and consider the natural double cover of $(G^\bullet)^{\times m} \times (G^\circ)^{\times n}$, branching exactly as the spinor $[\prod_{p=1}^m \prod_{q=1}^n (\mathcal{S}(v_p^\bullet) - \mathcal{S}(v_q^\circ))]^{1/2}$. Following the detailed discussion in [16, Section 2.2], the expressions (2.3) are spinors on $[\prod_{p=1}^m \prod_{q=1}^n (\mathcal{S}(v_p^\bullet) - \mathcal{S}(v_q^\circ))]^{1/2}$. When working with mixed correlation of the kind of (2.3), the usual Kramers-Wannier duality (see again [14, Proposition 3.3]) implies G^\bullet and G° play equivalent roles.

Among all possible correlators of the form (2.3), consider the special case where one of the disorders $v^\bullet(c) \in G^\bullet$ and one of the spins $v^\circ(c) \in G^\circ$ are chosen to be neighbours in $\Lambda(G)$, linked by an edge identified with a corner $c \in \Upsilon(G)$. In that case, one can formally denote the *fermion* at c by

$$\chi_c := \mu_{v^\bullet(c)} \sigma_{v^\circ(c)}, \quad (2.4)$$

One can now use (2.3) to construct the Kadanoff-Ceva *fermionic observables*, in a purely combinatorial manner, by setting

$$X_\varpi(c) := \mathbb{E}[\chi_c \mu_{v_1^\bullet} \dots \mu_{v_{m-1}^\bullet} \sigma_{v_1^\circ} \dots \sigma_{v_{n-1}^\circ}]. \quad (2.5)$$

Given the above remarks, the fermionic observable $X_\varpi(c)$ is defined up to the sign, but its definition becomes fully legitimate when working in $\Upsilon_\varpi^\times(G)$. Around each quad $z = (v_0^\bullet, v_0^\circ, v_1^\bullet, v_1^\circ)$ (listing its vertices in counterclockwise order as in [12, Figure 3.A] or Figure 1), that Kadanoff-Ceva observables satisfy some very simple local linear equations, with coefficients depending only on the Ising coupling constant attached to the quad z . This propagation equation appeared in the works of [22], [52] and [45, Section 4.3]). Let us be more concrete. Let θ_z be the abstract angle corresponding to the parametrization (1.2) of the edge in G^\bullet attached to the quad z . Then for any triplet of corners c_{pq} (identified as $c_{pq} = (v_p^\bullet v_q^\circ)$), where the lifts of c_{pq} , $c_{p,1-q}$ and of $c_{1-p,q}$ to $\Upsilon_\varpi^\times(G)$ are neighbors, one has

$$X(c_{pq}) = X(c_{p,1-q}) \cos \theta_z + X(c_{1-p,q}) \sin \theta_z, \quad (2.6)$$

where . One can easily show that solutions to (2.6) are automatically spinors on $\Upsilon_\varpi^\times(G)$.

To conclude this reminder on Kadanoff-Ceva correlators, we recall the generalisation of the definition of the Dirac spinor η_c , that is a special solution to (2.6) *on isoradial grids*. Given any fixed embedding $\mathcal{S} : \Lambda(G) \rightarrow \mathbb{C}$ of $\Lambda(G)$ into the complex plane, denote (as in [20])

$$\eta_c := \varsigma \cdot \exp \left[-\frac{i}{2} \arg(\mathcal{S}(v^\bullet(c)) - \mathcal{S}(v^\circ(c))) \right], \quad \varsigma := e^{i\frac{\pi}{4}}, \quad (2.7)$$

where the pre-factor $\varsigma = e^{i\frac{\pi}{4}}$ is chosen for convenience. One can once again avoid the sign ambiguity in (2.7) by passing working on a double cover $\Upsilon^\times(G)$. In particular, the products $\eta_c X_\varpi(c) : \Upsilon_\varpi(G) \rightarrow \mathbb{C}$ are defined on $\Upsilon_\varpi(G)$ that only branches over ϖ . Note that below, we keep using the notation (2.7) even when \mathcal{S} is not isoradial grid.

2.2. Definition of an s -embeddings. We now present now concisely the embedding procedure introduced by Chelkak in [13, Section 6] and then developed in greater details in [12]. One starts by recalling the definition of an s -embedding given in [12, Definition 2.1], using the Kadanoff-Ceva formalism. The general idea is to use a solution to (2.6) to construct some concrete embedding attached to the weighted graph.

Definition 2.1. Let (G, x) be a weighted planar graph with the combinatorics of the plane and fix $\mathcal{X} : \Upsilon^\times(G) \rightarrow \mathbb{C}$ one solution to the full system of equations (2.6) around each quad. We say that $\mathcal{S} = \mathcal{S}_\mathcal{X} : \Lambda(G) \rightarrow \mathbb{C}$ is an s -embedding of (G, x) associated to \mathcal{X} if for each $c \in \Upsilon^\times(G)$, we have

$$\mathcal{S}(v^\bullet(c)) - \mathcal{S}(v^\circ(c)) = (\mathcal{X}(c))^2. \quad (2.8)$$

For $z \in \diamond(G)$, the quadrilateral $\mathcal{S}^\diamond(z) \subset \mathbb{C}$ is the one delimited by the edges connecting the vertices $\mathcal{S}(v_0^\bullet(z)), \mathcal{S}(v_0^\circ(z)), \mathcal{S}(v_1^\bullet(z)), \mathcal{S}(v_1^\circ(z))$. The s -embedding \mathcal{S} is called proper if the quadrilaterals $\mathcal{S}^\diamond(z) = (\mathcal{S}(v_0^\bullet(z))\mathcal{S}(v_0^\circ(z))\mathcal{S}(v_1^\bullet(z))\mathcal{S}(v_1^\circ(z)))$ do not overlap with each other, and is called non-degenerate if no quads $\mathcal{S}^\diamond(z)$ degenerates to a segment. No convexity of the quads $\mathcal{S}^\diamond(z)$ is required.

It is not at automatic that, given any solution \mathcal{X} to (2.6), the obtained embedding $\mathcal{S}_\mathcal{X}$ is proper, meaning that finding a solution to (2.6) that leads to a non-degenerate proper picture is a non-trivial step. We can also extend the definition of \mathcal{S} to centres of quads of $\diamond(G)$, by setting as in [12, Equation (2.5)]

$$\begin{aligned} \mathcal{S}(v_p^\bullet(z)) - \mathcal{S}(z) &:= \mathcal{X}(c_{p0})\mathcal{X}(c_{p1}) \cos \theta_z, \\ \mathcal{S}(v_q^\circ(z)) - \mathcal{S}(z) &:= -\mathcal{X}(c_{0q})\mathcal{X}(c_{1q}) \sin \theta_z, \end{aligned} \quad (2.9)$$

where c_{p0} and c_{p1} (respectively, c_{0q} and c_{1q}) are neighbors on $\Upsilon^\times(G)$. The propagation equation (2.6) implies directly the consistency of both (2.8) and (2.9). From a concrete point of view (see Figure (1)), the image $\mathcal{S}^\diamond(z) \in \mathbb{C}$ of a combinatorial quad $z \in \diamond(G)$ into the complex plane in the embedding \mathcal{S} is a *quadrilateral tangential to a circle centred* at the point $\mathcal{S}(z)$ given by (2.9). The position of the point $\mathcal{S}(z)$ also corresponds to the intersection of the four bisectors of the sides of the tangential quadrilateral $\mathcal{S}^\diamond(z)$. The radius r_z of that circle can be recovered using the values of \mathcal{X} , using e.g. [12, Equation (2.7)]. In the rest of the paper, given $\delta' > 0$, we say that the tangential quadrilateral $\mathcal{S}^\diamond(z)$ is δ' -fat if $r_z \geq \delta'$. Denoting by $\phi_{v,z}$ the half-angle of the quad $\mathcal{S}^\diamond(z)$ at $\mathcal{S}(v)$, it is possible to reconstruct the

abstract Ising weight θ_z (in the parametrization (1.2)) from the angles in the image of $\mathcal{S}^\diamond(z) \subset \mathbb{C}$ using the formula [12, Equation (2.8)]

$$\tan \theta_z = \left(\frac{\sin \phi_{v_0^\bullet, z} \sin \phi_{v_1^\bullet, z}}{\sin \phi_{v_0^\diamond, z} \sin \phi_{v_1^\diamond, z}} \right)^{1/2}. \quad (2.10)$$

In the s -embedding framework, it is the large scale properties of the origami map attached to an embedding that indicate whether one can interpret or not a planar graph equipped with Ising weights as a (near)-critical system or not. One recalls its definition coming from [12, Definition 2.2] (see also [36, 19] for the general definition in the dimer context).

Definition 2.2. Given $\mathcal{S} = \mathcal{S}_\mathcal{X}$, one defines (up to a global additive constant) the *origami* function denoted by $\mathcal{Q} = \mathcal{Q}_\mathcal{X} : \Lambda(G) \rightarrow \mathbb{R}$, as a real-valued function, by setting its increments between two neighbours $v^\bullet(c)$ and $v^\diamond(c)$ to be

$$\mathcal{Q}(v^\bullet(c)) - \mathcal{Q}(v^\diamond(c)) := |\mathcal{X}(c)|^2 = |\mathcal{S}(v^\bullet(c)) - \mathcal{S}(v^\diamond(c))|. \quad (2.11)$$

We will often shorten $|\mathcal{X}(c)|^2 = \delta_c$ the length of the edge of $\Lambda(G)$ attached to the corner c .

Once again, the propagation equation (2.6) implies the consistency of Definition 2.2. We will detail below (following e.g. [12, Section 2.3] and [36, Section 7]) how one can extend the map \mathcal{Q} into a piecewise linear manner to the *entire* plane and not only to edges of $\Lambda(G)$.

Definition 2.3 (Assumption UNIF(δ)). We say that \mathcal{S} satisfies the assumption $\text{UNIF}(\delta) = \text{UNIF}(\delta, r_0, \theta_0)$ for some parameters δ, r_0, θ_0 if all edge-lengths in \mathcal{S} are comparable to δ , meaning that for any neighbouring $v^\bullet \in G^\bullet$ and $v^\diamond \in G^\diamond$ one has

$$r_0^{-1} \cdot \delta \leq |\mathcal{S}(v^\bullet) - \mathcal{S}(v^\diamond)| \leq r_0 \cdot \delta, \quad (2.12)$$

and all the geometric angles in the quads \mathcal{S} are bounded from below by θ_0 .

In particular, it is easy to see that in the general formalism introduced in Section 2.1 to define in full generality the scale of an s -embedding, there exist constants $\kappa < 1$ and C_0 , only depending on r_0, θ_0 such that grids satisfying the assumption $\text{UNIF}(\delta, r_0, \theta_0)$ have to satisfy the assumptions $\text{LIP}(\kappa, \delta)$ and $\text{EXP-FAT}_0(\delta, \rho(\delta))$ hold for some scale $\rho(\delta) = C_0 \cdot \delta$.

2.3. S-holomorphic functions and associated primitives. Let us recall now the notion of *s-holomorphic functions*, generalized to s -embeddings in [12], and originally introduced for the critical square lattice by Smirnov [54, Definition 3.1] and on isoradial grids by Chelkak and Smirnov in [20, Definition 3.1]. This notion is the key ingredient in the use of discrete complex analysis techniques for the Ising and dimer models. We recall the general definition of an s -holomorphic functions, as stated in [12, Definition 2.4]. In what follows, let $\text{Proj}[\cdot, \eta \mathbb{R}]$ stands for the usual projection the line $\eta \mathbb{R}$.

Definition 2.4. A function F defined on a subset of $\diamond(G)$ is called s -holomorphic if for each pair of adjacent quads $z, z' \in \diamond(G)$ separated by the edge $[\mathcal{S}(v^\diamond(c)); \mathcal{S}(v^\bullet(c))]$ of \mathcal{S} attached to the corner c , one has

$$\text{Proj}[F(z), \eta_c \mathbb{R}] = \text{Proj}[F(z'), \eta_c \mathbb{R}]. \quad (2.13)$$

The previous definition provides a direct link between real valued solutions to (2.6) and complex valued s -holomorphic functions. This link was originally presented in [12, Proposition 2.5] and in [19, Appendix].

Proposition 2.5. *Let $\mathcal{S} = \mathcal{S}_X$ be a proper s -embedding and F an s -holomorphic on $\diamondsuit(G)$. Given $z \in \diamondsuit(G)$, a corner $c \in \Upsilon^\times(G)$ belonging to the quad z , one can define the spinor X at $c \in \Upsilon^\times$ by the formula*

$$\begin{aligned} X(c) &:= |\mathcal{S}(v^\bullet(c)) - \mathcal{S}(v^\circ(c))|^{\frac{1}{2}} \cdot \operatorname{Re}[\bar{\eta}_c F(z)] \\ &= \operatorname{Re}[\bar{\varsigma} \mathcal{X}(c) \cdot F(z)] = \bar{\varsigma} \mathcal{X}(c) \cdot \operatorname{Proj}[F(z); \eta_c \mathbb{R}]. \end{aligned} \quad (2.14)$$

Then the function $c \mapsto X(c)$ satisfies the propagation equation (2.6) around the quad z . Conversely, given $X : \Upsilon^\times(G) \rightarrow \mathbb{R}$ a real valued solution to (2.6), there exists a unique s -holomorphic function F such that the identity (2.14) is fulfilled.

Provided the functions F and X are linked by (2.14), one can reconstruct the value of F at $z \in \diamondsuit(G)$ from the values of X at any pair of corners $c_{pq}(z) \in \Upsilon^\times(G)$ and the geometry of \mathcal{S} , e.g. using the formula [12, Corollary 2.6]

$$F(z) = -i\varsigma \cdot \frac{\overline{\mathcal{X}(c_{01}(z))} X(c_{10}(z)) - \overline{\mathcal{X}(c_{10}(z))} X(c_{01}(z))}{\operatorname{Im}[\overline{\mathcal{X}(c_{01}(z))} \mathcal{X}(c_{10}(z))]} \quad (2.15)$$

In the s -embedding framework, the behavior of the scaling limit of s -holomorphic functions is determined by their local equations together with their boundary conditions. This can be understood starting from two different integration procedures at the discrete level. The first is a standard extension of the integration procedure for discrete holomorphic functions to the s -embedding framework, now taking into account the presence of the origami map. The second is a generalization of Smirnov's primitive of the square of an s -holomorphic function. The former is studied in detail in [19, Proposition 6.15] and will be useful for deriving the local regularity theory for discrete functions and their local equations in the limit, while the latter was introduced by Smirnov in [54] on the critical square lattice to identify discrete Riemann-Hilbert boundary conditions appearing in the Ising model. Let us start with the primitive $I_{\mathbb{C}}$. Given an s -holomorphic function F on $\diamondsuit(G)$, one can define it (up to a global additive constant) as in [12, Section 2.3].

$$I_{\mathbb{C}}[F] := \int (\bar{\varsigma} F d\mathcal{S} + \varsigma \overline{F} d\mathcal{Q}). \quad (2.16)$$

Let $v_{1,2}^\bullet, v_{1,2}^\circ$ be vertices of the quad $z \in \diamondsuit(G)$. Then one has for $\star \in \{\bullet, \circ\}$

$$I_{\mathbb{C}}[F](v_2^\star) - I_{\mathbb{C}}[F](v_1^\star) = \bar{\varsigma} F(z) [\mathcal{S}(v_2^\star) - \mathcal{S}(v_1^\star)] + \varsigma \overline{F(z)} [\mathcal{Q}(v_2^\star) - \mathcal{Q}(v_1^\star)]. \quad (2.17)$$

The extension of the origami map presented in Section 2.4 also extends the definition of (2.16) to the entire complex plane. For the notion of primitive of square H_X , one can start with a purely combinatorial definition tied to the Kadanoff-Ceva formalism, which doesn't require any particular embedding into the plane, provided one works with a spinor X satisfying (2.6). This generalization of the original work of Smirnov, can be found in the following form in [12, Definition 2.8].

Definition 2.6. Given X a spinor on $\Upsilon^\times(G)$ satisfying (2.6), one can define the function H_X up to a global additive constant on $\Lambda(G) \cup \diamondsuit(G)$ by setting

$$\begin{aligned} H_X(v_p^\bullet(z)) - H_X(z) &:= X(c_{p0}(z))X(c_{p1}(z))\cos\theta_z, \quad p = 0, 1, \\ H_X(v_q^\circ(z)) - H_X(z) &:= -X(c_{0q}(z))X(c_{1q}(z))\sin\theta_z, \quad q = 0, 1, \\ H_X(v_p^\bullet(z)) - H_X(v_q^\circ(z)) &:= (X(c_{pq}(z)))^2, \end{aligned} \quad (2.18)$$

similarly to (2.8) and (2.9).

The consistency of the above definition follows from (2.6). Passing to an s -embedding \mathcal{S} of the graph (G, x) , the correspondence between X and F recalled in Proposition 2.5 allows to interpret H_X via the s -holomorphic function F attached to X . More precisely, one can set as in [12, Equation (2.17)]

$$H_F := \int \operatorname{Re}(\bar{\zeta}^2 F^2 d\mathcal{S} + |F|^2 d\mathcal{Q}) = \int (\operatorname{Im}(F^2 d\mathcal{S}) + \operatorname{Re}(|F|^2 d\mathcal{Q})), \quad (2.19)$$

on $\Lambda(G) \cup \diamondsuit(G)$. The extension of \mathcal{Q} described below allows to extend H_F in a piece-wise affine manner to the entire plane (here one has to be careful as the extension will happen on each faces of the associated t -embedding $\mathcal{T} = \mathcal{S}$ -see [19, Proposition 3.10]). The next lemma links the definitions (2.18) and (2.19), proving that they are in fact the *same* function.

Lemma 2.7. [12, Lemma 2.9] *Let F be defined $\diamondsuit(G)$ and X be defined on $\Upsilon^\times(G)$ related by the identity (2.14). Then, the functions H_F and H_X coincide up to a global additive constant.*

If \mathcal{S} is an isoradial grid, the origami map \mathcal{Q} is constant on both G^\bullet and G° (as all the edges of the quads $\mathcal{S}^\circ(z)$ share the same length), thus H_F is the primitive of $\operatorname{Im}[F^2 d\mathcal{S}]$, recovering the original definition given in [20, Section 3.3].

2.4. Bosonization of the Ising model, S-graphs and random walks. To identify the scaling limit of the full-plane energy observable, we will identify its primitive as a full-plane Green function on an S-graph. The name S-graphs, coined in [12, Section 2.3], refers to a special case of the so-called T-graphs introduced in [37] and extensively studied in the dimer context (see, e.g., [8, 19]), as they provide the natural framework for studying gradients of dimer observables.

In particular, we start our reminder with the standard way of viewing an Ising model as a dimer model, following the bosonization procedure introduced in [24] (see also [56, Section 2.3.3] for a complete exposition). We advise the reader to follow this section together with Figures 2 and 3. Given a planar graph (G, x) equipped with the Ising model, one can construct a dimer model on the bipartite graph $\Upsilon^\bullet(G) \cup \Upsilon^\circ(G)$ with simple dimer weights. Each quad $z \in \diamondsuit$ is split into four triangles, each containing a pair of neighboring vertices $v^\bullet, v^\circ \in \Lambda(G)$ and the center of the quad z . One can then define a bipartite coloring $B \cup W$ of the faces of this subdivision into two colors: the black ones $b \in B$ and the white ones $w \in W$.

A dimer configuration on $B \cup W$ is a perfect matching of $B \cup W$, where the weight $K(w, b)$ represents the multiplicative cost of a match between adjacent faces $w \in W$ and $b \in B$. When constructing a dimer model from an Ising model, the weights assigned to each pair of adjacent faces $b \sim w$ are given by

$$K(w, b) = \begin{cases} \cos(\theta_z) & \text{if } w, b \text{ belong to the same quad } z \text{ and share a vertex of } G^\bullet, \\ \sin(\theta_z) & \text{if } w, b \text{ belong to the same quad } z \text{ and share a vertex of } G^\circ, \\ 1 & \text{otherwise.} \end{cases}$$

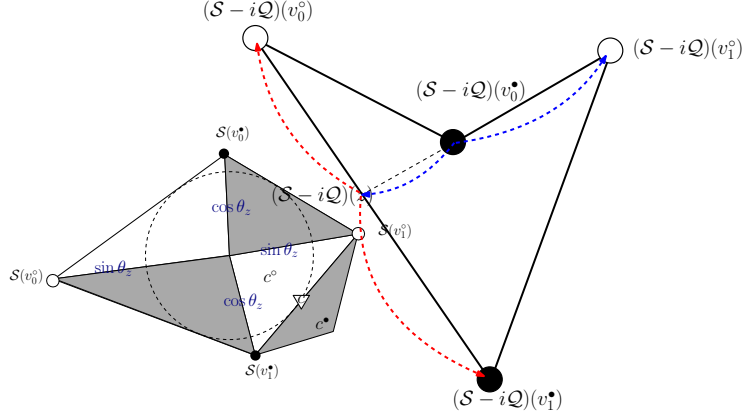


FIGURE 2. (Left) Bosonization of the Ising model as a dimer model: each quad $z \in \diamondsuit(G)$ is split into four triangles, colored in a bipartite fashion between black faces B and white faces W . The dimer weight $K(w, b)$ of the match between faces $b \in B$ and $w \in W$ is either $\cos(\theta_z)$, $\sin(\theta_z)$, or 1, depending on whether the faces belong to the same quad or not. To each corner $c \in \Upsilon$, one attaches two neighboring faces $c^\circ \in W$ and $c^\bullet \in B$, which allows computing the associated dimer *origami square root* $\eta_c^\bullet = \eta_{c^\circ}^\bullet := \bar{\zeta} \eta_c$ using (2.7). (Right) A piece of the S-graph $\mathcal{S} - iQ$: the black triangle $(\mathcal{S}(v_0^\bullet)\mathcal{S}(v_1^\circ)\mathcal{S}(z))$ is mapped to the segment $[(\mathcal{S} - iQ)(z), (\mathcal{S} - iQ)(v_1^\circ)]$, which contains the point $(\mathcal{S} - iQ)(v_0^\bullet)$ in its interior. The *continuous-time directed* random walk $X_t^{(\alpha)}$ for $\alpha = \exp(-i\frac{\pi}{4})$ has nonzero jump rates from $(\mathcal{S} - iQ)(v_0^\bullet)$ to $(\mathcal{S} - iQ)(z)$ and $(\mathcal{S} - iQ)(v_1^\circ)$ (see Definition 2.9), as indicated by the dashed oriented arrows. The invariant measure $\mu^{(\alpha)}(v_0^\bullet)$ equals the area of the triangle $(\mathcal{S}(v_0^\bullet)\mathcal{S}(v_1^\circ)\mathcal{S}(z))$.

When \mathcal{S} is a proper s -embedding, the splitting of quads $\mathcal{S}^\circ(z)$ into four triangles defines a *t-embedding*, where each face is a triangle with vertices consisting of one vertex of $\mathcal{S}(G^\circ)$, one vertex of $\mathcal{S}(G^\bullet)$, and the center of the quad $\mathcal{S}(z)$. Given a vertex $v \in \mathcal{S}(\Lambda(G) \cup \diamondsuit(G))$ and a face $b \in B$ containing v , let $\theta(v, b)$ denote the geometric angle of the triangular face b at v . Then $\sum_{v \in b} \theta(v, b) = \pi$. A similar statement holds for the sum of the angles $\theta(v, w)$ attached to white faces containing v . It is straightforward to check that the edge weight $K(w, b)$ is *gauge equivalent* (see, e.g., [36, Section 7] or [19, Section 8.2]) to the length of the segment $(wb)^*$ separating the faces w and b in \mathcal{S} .

We can now define the following construction to extend the origami map to the entire plane:

- Consider $\mathcal{S} : \Lambda(G) \cup \diamond(G) \rightarrow \mathbb{C}$ as a t -embedding \mathcal{T} . In this setup, each corner $c \in \Upsilon(G)$ belongs to two distinct faces $c^\bullet \in B$ and $c^\circ \in W$ of \mathcal{T} . Set

$$\eta_{c^\bullet}^{\mathfrak{d}} = \eta_{c^\circ}^{\mathfrak{d}} := \bar{\zeta} \eta_c, \quad (2.20)$$

where η_c is defined by (2.7). Then the function $\eta^{\mathfrak{d}} : B \cup W \rightarrow \mathbb{T}$ is an *origami square root* in the sense of [19, Definition 2.4].

- One can define the origami map *on the entire complex plane*, up to a global additive constant, by setting for any z' in the \mathcal{S} -plane

$$d\mathcal{Q}(z') := \begin{cases} (\eta_{c^\circ}^{\mathfrak{d}})^2 dz' & \text{if } (z' \in c^\circ) \in W, \\ (\eta_{c^\bullet}^{\mathfrak{d}})^2 dz' & \text{if } (z' \in c^\bullet) \in B. \end{cases}$$

Along the edges of $\Lambda(G)$, this definition agrees with that given in Definition 2.2.

From the t -embedding $\mathcal{T} = \mathcal{S}$, one can construct a family of graphs indexed by $\alpha \in \mathbb{T}$, called S-graphs. These form a special subclass of the so-called t -graphs associated with t -embeddings, studied in more detail, for instance, in [12, Section 2.3]. The relevance of T-graphs lies in the fact that s -holomorphic functions on an s -embedding \mathcal{S} can be viewed as gradients of harmonic functions on S-graphs.

Definition 2.8. Given $\mathcal{S} = \mathcal{S}_\chi$ a non-degenerate proper s -embedding, the associated origami map $\mathcal{Q} = \mathcal{Q}_\chi$, and an unimodular number $\alpha \in \mathbb{T}$, we call $\mathcal{S} + \alpha^2 \mathcal{Q} : \Lambda(G) \rightarrow \mathbb{C}$ an S-graph associated to \mathcal{S} . An S-graph is called non-degenerate if for $v \neq v'$, one has $(\mathcal{S} + \alpha^2 \mathcal{Q})(v) \neq (\mathcal{S} + \alpha^2 \mathcal{Q})(v')$, which is equivalent to requiring that no white triangles $w \in W$ of \mathcal{T} is mapped to a single point in $\mathcal{S} + \alpha^2 \mathcal{Q}$.

From a geometrical standpoint, the S-graph has the following features:

- For $w = c^\circ \in W$, the white face $\mathcal{T}(w)$ is mapped to a triangle, which is a translate of $(1 + (\alpha \eta_{c^\circ}^{\mathfrak{d}})^2) \mathcal{T}(w)$. The orientations of these two triangles are the same.
- For $b = c^\bullet \in B$, the black face $\mathcal{T}(b)$ is mapped to a segment, which is a translate of $2 \text{Proj}[\mathcal{T}(b); \alpha \eta_{c^\bullet}^{\mathfrak{d}} \mathbb{R}]$.
- The S-graph is degenerate for $\alpha \in \mathbb{T}$ if and only if there exists an edge $[\mathcal{S}(v^\circ), \mathcal{S}(v^\bullet)]$ of $\mathcal{S}(\Lambda(G))$ such that $\mathcal{S}(v^\bullet) - \mathcal{S}(v^\circ) \in -\alpha^2 \mathbb{R}_+$. This corresponds to the case $\alpha = \bar{\zeta} \eta_c$, where c is the corner attached to $[\mathcal{S}(v^\circ), \mathcal{S}(v^\bullet)]$. In that case, not only the segment $[\mathcal{S}(v^\circ), \mathcal{S}(v^\bullet)]$ but also the entire white face $c^\circ = w \in W$ of \mathcal{T} containing this segment is shrunk to a point.
- From a more hands-on perspective (see, e.g., [19, Definition 4.2]), an S-graph with possibly degenerate faces can be seen as a disjoint, locally finite union of open segments and single points, called *degenerate*, such that:
 - each endpoint of an open segment either lies *strictly* inside another segment or corresponds to a *degenerate face*;
 - each degenerate face is the endpoint of $3 + m$ open segments, among which three are called outgoing segments and are not contained in a half-plane.

Let us now fix some $\alpha \in \mathbb{T}$ and some S-graph in the full plane $\mathcal{S} + \alpha^2 \mathcal{Q}$. One can define some continuous time random walk on this S-graph, following [19, Definitions 4.4 and 4.6].

Definition 2.9. Let $X_t = X_t^{(\alpha)}$ be the continuous-time random walk defined on the vertices of $\mathcal{S} + \alpha^2 \mathcal{Q}$ according to the following transition rates $q^{(\alpha)}$:

- For any non-degenerate vertex v , there exists a unique open segment $(v^-, v^+) \in \mathcal{S} + \alpha^2 \mathcal{Q}$ such that $v \in (v^-, v^+)$. Set

$$q^{(\alpha)}(v \rightarrow v_k) := \frac{1}{|v^\pm - v| \cdot |v^+ - v^-|}, \quad (2.21)$$

and all other transition rates vanish.

- If v is a degenerate vertex corresponding to a shrunk white face $w \in W$, let $b_1, b_2, b_3 \in B$ be the three black faces surrounding w . These black faces are mapped, respectively, by $\mathcal{S} + \alpha^2 \mathcal{Q}$ to the segments $(v, v_1), (v, v_2), (v, v_3)$ in the $\mathcal{S} + \alpha^2 \mathcal{Q}$ plane. In this case, set

$$q^{(\alpha)}(v \rightarrow v_k) := \frac{m_k}{|v_k - v|^2}, \quad m_k := \frac{S_{(b_k)}}{S_{(b_1)} + S_{(b_2)} + S_{(b_3)}}, \quad (2.22)$$

where $S_{(b)}$ is the area of the black triangle $b \in B$.

With the jump rates of the directed random walk defined above, both coordinates of the random process $(\mathcal{S} + \alpha^2 \mathcal{Q})(X_t)$ and the process $|(\mathcal{S} + \alpha^2 \mathcal{Q})(X_t)|^2 - t$ are martingales. The transition rates are normalized so that, for each non-degenerate vertex v , the expected time to exit v corresponds to the expected exit time of a one-dimensional Brownian motion starting at v and moving along the segment (v^-, v^+) until it reaches $\{v^-, v^+\}$. The jump rates also define a $\Delta^{(\alpha)}$ -Laplacian for a function H on the vertices of $\mathcal{S} + \alpha^2 \mathcal{Q}$ by setting

$$\Delta^{(\alpha)}[H](v) := \sum_{v_k \sim v} q^{(\alpha)}(v \rightarrow v_k) (H(v_k) - H(v)), \quad (2.23)$$

where $v_k \sim v$ if and only if $q^{(\alpha)}(v \rightarrow v_k) \neq 0$.

When the associated s -embedding does not degenerate at large scale, the random walk $X_t^{(\alpha)}$ defined above shares several properties with the standard balanced random walk on \mathbb{Z}^2 . More precisely, under the assumption $\text{LIP}(\kappa, \delta)$, the random walk $X_t^{(\alpha)}$ satisfies the so-called *uniform crossing estimates* starting at some scale comparable to δ . More concretely, there exist constants $C(\kappa)$ and $p(\kappa) > 0$, depending only on κ (and not on δ), such that for any $r \geq C(\kappa)\delta$ and any annulus $A(r, 2r)$ covered by \mathcal{S} , one has

$$\mathbb{P}[X_t^{(\alpha)} \text{ makes a full turn in the annulus } A(r, 2r) \text{ without exiting it}] \geq p(\kappa). \quad (2.24)$$

One of the key ingredients in studying the behavior of the walk $X^{(\alpha)}$ is that its invariant measure $\mu = \mu^{(\alpha)}$ (which depends on α) admits a fully geometric interpretation in the geometry of \mathcal{S} . This fact, highlighted in [19, Corollary 4.9], reads as follows. Let $v \in \mathcal{S} + \alpha^2 \mathcal{Q}$; then the following holds:

- If v is a non-degenerate vertex, let $b^{(\alpha)}(v)$ be the unique black face $b \in B$ of \mathcal{T} such that v lies *inside* the open segment $(\mathcal{S} + \alpha^2 \mathcal{Q})(b)$. Set

$$\mu^{(\alpha)}(v) := S_{(b^{(\alpha)}(v))}. \quad (2.25)$$

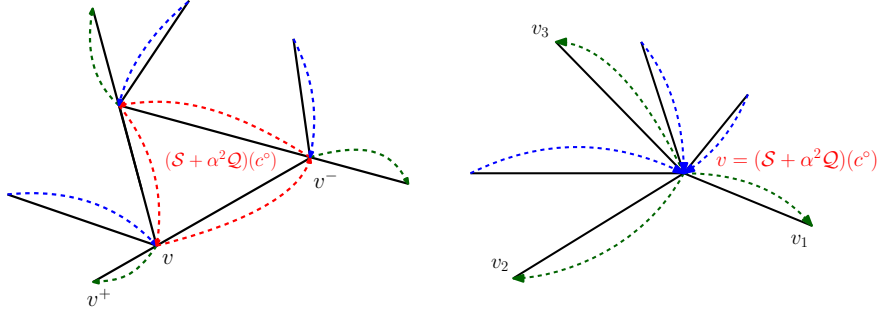


FIGURE 3. (Left) Transitions in a non-degenerated S-graph $\mathcal{S} + \alpha^2 \mathcal{Q}$. The allowed jump-rates of the directed random walk $X_t^{(\alpha)}$ are given by the dashed arrows. The triangle containing the 3 red arrows corresponds to the image of a face c^o . The walk can move from v to v^\pm if and only if $v \in (v^-; v^+)$. The variance of $X_t^{(\alpha)}$ is normalised so that the expected time for $X_t^{(\alpha)}$ to exit from v is equal to the expected time for one dimensional Brownian motion started at v along the segment $[v^-, v^+]$ to hit on of its extremities. (Right) Transitions in a degenerated S-graph $\mathcal{S} + \alpha^2 \mathcal{Q}$: When moving $\alpha \in \mathbb{T}$ up to value $\alpha = i \cdot \overline{\eta_{c^o}}$, the image of the white face c^o is shrunk to a single point. The three red transition rates become infinite as α approaches $i \cdot \overline{\eta_{c^o}}$, but their respective ratio remains finite and is given in the limit by ratios m_k in (2.22). This explains why the 3 outgoing $q^{(\alpha)}(v \rightarrow v_k)$ jump-rates from the degenerated vertex v are first multiplied by this limiting ratio then used the non-degenerated geometric formula. The invariant measure $\mu^{(\alpha)}(v)$ of the degenerate vertex v is the sum of the areas of the black faces surrounding c^o .

- If $v = (\mathcal{S} + \alpha^2 \mathcal{Q})(w)$ is a degenerate vertex, image of a shrunk face $w \in W$ of \mathcal{T} , let $b_1, b_2, b_3 \in B$ be the three black faces of \mathcal{T} surrounding w . Set

$$\mu^{(\alpha)}(v) := S_{(b_1)} + S_{(b_2)} + S_{(b_3)}. \quad (2.26)$$

Then the map $\mu = \mu^{(\alpha)}$ is invariant for the random walk $X^{(\alpha)}$. Moreover, when the S-graph has no degeneracies, the map $v \mapsto b^{(\alpha)}(v)$ is a bijection.

The relevance of the random walks on S-graphs for understanding s -holomorphic functions lies in the fact that projections of the primitive form $I_{\mathbb{C}}$ are harmonic on the corresponding S-graphs. To make this statement precise, we recall the link between s -holomorphic functions in the Ising context and the so-called t -holomorphic functions in the dimer context. Let F be an s -holomorphic function on $\diamondsuit(G)$. One can construct functions F^\bullet and F° associated with F , defined respectively on B and W , as follows:

- If $b = c^\bullet \in B$ is a black face attached to a corner $c \in \Upsilon$ in a quad z of $\mathcal{T} = \mathcal{S}_{\mathcal{X}}$, set

$$F^\bullet(b) := \text{Proj}[F(z); \eta_c \mathbb{R}] = \varsigma \frac{X(c)}{\mathcal{X}(c)} = \frac{X(c)\eta_c}{\delta_c^{1/2}}, \quad (2.27)$$

where X and F are related by (2.15).

- If $w = c^\circ \in W$ is a white face of a quad z in \mathcal{T} , set

$$F^\circ(w) := F(z). \quad (2.28)$$

One can then define a function $F_{\mathfrak{w}}$ on $B \cup W$ such that $(F_{\mathfrak{w}})|_B := \bar{\varsigma}F^\bullet$ and $(F_{\mathfrak{w}})|_W := \bar{\varsigma}F^\circ$. The function $F_{\mathfrak{w}}$ is then t -holomorphic for the origami square root $\eta^\mathfrak{d} : B \cup W \rightarrow \mathbb{T}$ of (2.20) in the sense of [19, Definition 3.2]. This means, in particular, that for any two white faces $w_1, w_2 \in W$ adjacent to a black face $b \in B$, one has

$$\text{Proj}[F_{\mathfrak{w}}(w_1); \eta_b^\mathfrak{d} \mathbb{R}] = \text{Proj}[F_{\mathfrak{w}}(w_2); \eta_b^\mathfrak{d} \mathbb{R}] = F_{\mathfrak{w}}(b),$$

which agrees with Definition 2.4.

We can now state a more concrete and crucial application of the random walk defined above. Given an s -holomorphic function F attached to a t -holomorphic function $F_{\mathfrak{w}}$ through the above correspondence, define

$$I_{\alpha \mathbb{R}}[\bar{\varsigma}F] := \text{Proj}[I_{\mathbb{C}}[\bar{\varsigma}F]; \alpha \mathbb{R}].$$

Then the function $\varsigma I_{\alpha \mathbb{R}}[\bar{\varsigma}F]$, which is $\varsigma \alpha \mathbb{R}$ -valued, when identified with $F_{\mathfrak{w}}$ on \mathcal{T} , is harmonic with respect to the directed continuous-time random walk $X_t^{(\alpha)}$ on the S-graph $\mathcal{S} + \alpha^2 \mathcal{Q}$. This fact is proven in [19, Proposition 4.15] and can be written as for every vertex $v \in \mathcal{S} + \alpha^2 \mathcal{Q}$

$$\Delta^{(\alpha)}[I_{\alpha \mathbb{R}}[\bar{\varsigma}F]](v) = 0.$$

2.5. Regularity theory for s-holomorphic functions. In this short subsection we recall in a concise way the regularity theory of s-holomorphic functions, which was developed in the dimer context in [19, Section 6.5]. The identification of the full-plane Green kernel and its derivative requires being able to extract some subsequential limits from discrete observables. In that context, the regularity theory of s-holomorphic functions requires adding to $\text{Lip}(\kappa, \delta)$ one (mild) geometrical constraints on potential local degeneracies of the embedding, following the framework introduced in [19, Assumption 1.2]. In that case, an s-holomorphic function F satisfies some standard Harnack-type estimate that controls $|F|$ via the oscillations of $I_{\alpha \mathbb{R}}[\bar{\varsigma}F]$, except in some pathological scenario where the discrete functions blow up exponentially fast in δ^{-1} .

Theorem 2.1. [19, Theorem 6.17] *For each fixed $\kappa < 1$, there exist constants $\gamma_0 = \gamma_0(\kappa) > 0$ and $C_0 = C_0(\kappa) > 0$ such that the following alternative holds. Let F be a s-holomorphic function defined in a ball of radius r drawn over an s-embedding \mathcal{S} satisfying the assumption $\text{Lip}(\kappa, \delta)$ and some $\alpha \in \mathbb{T}$. Then, provided that $r \geq \text{cst} \cdot \delta$ for a constant depending only on κ , one has the alternative*

$$\begin{aligned} \text{either } \max_{\{z: \mathcal{S}(z) \in B(u, \frac{1}{2}r)\}} |F| &\leq C_0 r^{-1} \cdot |\text{osc}_{\{v: \mathcal{S}(v) \in B(u, r)\}} I_{\alpha \mathbb{R}}[\bar{\varsigma}F]|, \\ \text{or } \max_{\{z: \mathcal{S}(z) \in B(u, \frac{3}{4}r)\}} |F| &\geq \exp(\gamma_0 r \delta^{-1}) \cdot C_0 r^{-1} |\text{osc}_{\{v: \mathcal{S}(v) \in B(u, r)\}} I_{\alpha \mathbb{R}}[\bar{\varsigma}F]|. \end{aligned}$$

Remark 2.10. We will use the first alternative of Theorem 2.1 to deduce that some properly scaled s-holomorphic functions F^δ form a precompact family (in the topology of uniform convergence on compacts) as $\delta \rightarrow 0$. Indeed, it is enough to prove that one of the associated primitives $I_{\alpha \mathbb{R}}[\bar{\varsigma}F]$ is bounded, together with the assumption $\text{Exp-FAT}_0(\delta, \rho(\delta))$, to deduce that the observables F are $\beta(\kappa)$ -Hölder (see [12, Theorem 2.18]) on arbitrarily small scales as $\delta \rightarrow 0$.

2.6. Subsequential limits of s -holomorphic functions. Let us now discuss the behavior of subsequential limits of s -holomorphic functions under the general hypothesis $\text{LIP}(\kappa, \delta)$, which was first studied in greater detail in [12, Section 2.7]. We consider a sequence of proper s -embeddings $(\mathcal{S}^\delta)_{\delta>0}$, each satisfying the assumption $\text{LIP}(\kappa, \delta)$ as $\delta \rightarrow 0$ for the *same* constant $\kappa < 1$, and whose images cover a ball $U = B(u, r) \subset \mathbb{C}$. Recall that the functions $(\mathcal{Q}^\delta)_{\delta>0}$ are all κ -Lipschitz starting at some scale $O(\delta)$ and are defined up to an additive constant. Thus, there exists a subsequence $\delta_k \rightarrow 0$ and a κ -Lipschitz function $\vartheta : U \rightarrow \mathbb{R}$ such that, uniformly on compact subsets of the ball U ,

$$\mathcal{Q}^{\delta_k} \circ (\mathcal{S}^{\delta_k})^{-1} \rightarrow \vartheta. \quad (2.29)$$

In the case where the first alternative of Theorem 2.1 holds, and passing to a subsequence as in (2.29), let $f : U \rightarrow \mathbb{C}$ be a subsequential limit of s -holomorphic functions F^δ on \mathcal{S}^δ . Then, following [12, Proposition 2.21] and keeping $\varsigma = e^{i\frac{\pi}{4}}$ as in (2.7), the differential form $\frac{1}{2}(\bar{\varsigma}f dz + \varsigma\bar{f} d\vartheta)$ is closed, as a natural counterpart of (2.16). Moreover, with a proper choice of additive constants, the associated functions H_{F^δ} also converge in turn to $h := \int (\text{Im}(f^2 dz) + |f|^2 d\vartheta)$ uniformly on compact subsets.

Understanding in practice the closedness of $\frac{1}{2}(\bar{\varsigma}f dz + \varsigma\bar{f} d\vartheta)$ is not straightforward, and it makes it a priori difficult to interpret the local relation satisfied by f . In [12, Section 2.7], a more convenient description of this local relation was proposed by passing to a conformal parametrization of a suitably chosen surface in Minkowski space $\mathbb{R}^{2,1}$, equipped with the inner product of signature $(+, +, -)$ (or $(2, 1)$). Since the function ϑ is κ -Lipschitz, and thus differentiable almost everywhere, one can consider (as in [12, Equation (2.26)]) an orientation-preserving *conformal parametrization* of the space-like surface $(z, \vartheta(z))_{z \in U}$, equipped with the positive metric induced from the ambient Minkowski space $\mathbb{R}^{2,1}$.

$$\mathbb{D} \ni \zeta \mapsto (z, \vartheta) \in U \times \mathbb{R} \subset \mathbb{C} \times \mathbb{R} \cong \mathbb{R}^{2+1} \quad (2.30)$$

As first noticed in [12, below Equation (2.26)], in the case where the function ϑ is a smooth, the angles (measured in $\mathbb{R}^{2,1}$) of infinitesimal increments are preserved by (2.30) if and only if everywhere in \mathbb{D} , one has the following relation (see [12, Equation (2.27)])

$$z_\zeta \bar{z}_\zeta = (\vartheta_\zeta)^2 \quad \text{and} \quad |z_\zeta| > |\vartheta_\zeta| \geq |\bar{z}_\zeta|, \quad (2.31)$$

where $z_\zeta := \partial z / \partial \zeta$ (similarly, \bar{z}_ζ and ϑ_ζ) stands for the usual Wirtinger derivatives in the ζ variable. In general, one cannot assume that ϑ is smooth, but still note that the conformal parametrisation (2.31) is equivalent to the *quasi-conformal* parametrisation $z \mapsto \zeta(z)$, meaning here it is a solution to the Beltrami equation

$$\zeta_{\bar{z}} = \mu(z) \zeta_z, \quad (2.32)$$

(or in an equivalent way to $\bar{z}_\zeta = -\overline{\mu(z)} z_\zeta$), with the Beltrami coefficient μ given by the relation

$$\frac{\bar{\mu}}{1 + |\mu|^2} = -\frac{\vartheta_z^2}{1 - 2|\vartheta_z|^2}. \quad (2.33)$$

Following [12, Equation (2.30)], one gets that $|\mu| \leq \text{cst}(\kappa) < 1$. This allows to:

- Compute the Beltrami coefficient $\mu \in L^\infty$ in (2.33) *almost everywhere* in the plane, as ϑ is differentiable almost everywhere (with respect to the Lebesgue measure).

- Use the Ahlfors-Bers's measurable Riemann mapping theorem [5, Chapter 5] to construct a solution to (2.32), providing a quasi-conformal uniformisation $\zeta : U \mapsto \mathbb{D}$ such that the relation (2.31) holds almost everywhere in \mathbb{D} .

Note that one can extend such a parametrisation to the entire surface $(z, \vartheta)_{z \in \mathbb{C}}$. Up to fixing the image and the (positive) Jacobian at the origin $\zeta = 0$, there exist one unique full-plane parametrization (again by [5, Chapter 5]). In the $\zeta \in \mathbb{D}$ parametrisation, there exist a convenient change of variable for the function f (suggested first in [12, Equation (2.28)]), by setting

$$\phi(\zeta) := \bar{\zeta}f(z(\zeta)) \cdot (z_\zeta)^{1/2} + \zeta\overline{f(z(\zeta))} \cdot (\bar{z}_\zeta)^{1/2} \quad (2.34)$$

With this change of variables, $I_{\mathbb{C}}[f] := \int \bar{\zeta}f(z)dz + \zeta\overline{f(z)}d\vartheta$ is now expressed as

$$g(\zeta) = \int^{z(\zeta)} \bar{\zeta}\phi(\zeta) \cdot z_\zeta^{\frac{1}{2}} d\zeta + \zeta\overline{\phi(\zeta)} \cdot (\bar{z}_\zeta)^{\frac{1}{2}} d\bar{\zeta}. \quad (2.35)$$

It is easy to compute the associated Wirtinger derivatives in the ζ variable (see [18, Proposition 2.21]), and using the relation (2.31), one can deduce that g satisfies a *conjugate* Beltrami equation (almost everywhere in \mathbb{D})

$$g_{\bar{\zeta}} = i\bar{\nu} \cdot \overline{g_\zeta} \quad \text{with} \quad \nu := -\frac{(\bar{z}_\zeta)^{\frac{1}{2}}}{(z_\zeta)^{\frac{1}{2}}} = -\frac{\vartheta_\zeta}{z_\zeta} \quad (2.36)$$

with a Beltrami coefficient ν again bounded away from 1, with a bound only depending on κ (see [12, Equation (2.30)] or [18, Proposition 2.21]). The focus on the function g is two fold: beyond satisfying (2.36), it is the primitive of some continuous differential form and hence inherits some additional regularity. Provided that f is locally bounded, one can deduce that

- The function g has a distortion bounded by $\frac{1+\kappa}{1-\kappa}$ (see e.g. [5, Equation (2.27)] for exact definitions).
- The function g also belongs to $W_{\text{loc}}^{1,2}$ as recalled in [40, Section 2.5].

As a combination of the two previous observations, one can apply the Stoïlov factorisation recalled in [5, Corollary 5.3.3] which allows factories $g = \underline{g} \circ p$ with $p : U \rightarrow U$ some $\beta(\kappa)$ -Hölder homeomorphism and \underline{g} an holomorphic function.

Let us also mention the special case when the function ϑ is smooth. In that setup, the function ϕ satisfies the *massive Dirac equation* [12, Section 2.7]

$$\phi_{\bar{\zeta}} = i \cdot m(\zeta) \cdot \overline{\phi}(\zeta) \quad \text{where} \quad m(\zeta) = \frac{z_{\zeta\bar{\zeta}}}{2(z_\zeta z_{\bar{\zeta}})^{\frac{1}{2}}} = \frac{(|\vartheta_{\zeta\bar{\zeta}}|^2 - |z_{\zeta\bar{\zeta}}|^2)^{\frac{1}{2}}}{2(|z_\zeta| - |z_{\bar{\zeta}}|)}. \quad (2.37)$$

One has $m(\zeta) = \frac{1}{2}H(\zeta)l(\zeta)$ where $H(\zeta)$ and $l(\zeta)$ are respectively the *mean curvature* and the *metric element* of the surface $(z, \vartheta) \subset \mathbb{R}^{(2,1)}$. This explains the special role of maximal surfaces where the function ϕ is holomorphic in the ζ parametrisation and recovers some conformal invariance.

2.7. The generalised Green function for Beltrami equations. The discussion in the previous section shows that the scaling limit of s -holomorphic functions under the assumption $\text{LIP}(\kappa, \delta)$ can be described as solutions to conjugate Beltrami equations. The purpose of the present section is to provide a more detailed description of the limiting two-point correlator in the full plane. We begin with an informal discussion in the “small” origami setting, already studied in [19], where

$\vartheta \equiv 0$. Let $F_{(a^\delta)}$ denote the complexified s -holomorphic function (except at the corner a^δ) associated with the fermion defined in Section 3.1. After an appropriate rotation and scaling of \mathcal{S}^δ , the discrete form $I_{\mathbb{C}}[F_{(a^\delta)}]$, defined in (2.16), satisfies the following properties: it is locally well defined away from a^δ and has a monodromy $2i$ when winding around a^δ . On a suitably chosen S-graph, the function $\text{Re}[I_{\mathbb{C}}[F_{(a^\delta)}]]$ is well defined and discrete harmonic away from a^δ , and has logarithmic growth near the origin and at infinity.

Since the graphs \mathcal{S}^δ and $\mathcal{S} + \alpha^2 \mathcal{Q}^\delta$ are close to each other in the small origami regime ($\mathcal{Q}^\delta \rightarrow 0$), the continuous analogue $I[f_{(a)}]$ of $I_{\mathbb{C}}[F_{(a^\delta)}]$ should be a locally closed form on $\mathbb{C} \setminus \{a\}$, whose real part is harmonic, have a monodromy $2i$ when winding around a , and have logarithmic growth near a and infinity. Since f_a is holomorphic away from a , these constraints determine it uniquely as

$$I[f_{(a)}](z) = \frac{1}{\pi} \log(z - a) + \text{cst.}$$

Beyond the small origami case, an analogous characterization of $I[f_{(a)}]$ holds when the limiting function $\vartheta \equiv 0$ is replaced by a generic κ -Lipschitz function ϑ . More precisely, there exists (up to an additive constant) a unique function satisfying natural generalizations of the above properties. The following theorem formalizes this statement and describes the scaling limit of the two-point fermionic correlator.

Theorem 2.11. *Let ϑ be $\kappa < 1$ -Lipschitz function in \mathbb{C} , $\eta \in \mathbb{C}$ and $a \in \mathbb{C}$. Up to additive constant, there exists one unique function $z \mapsto g_{\vartheta,(a)}^{[\eta]}(z)$ that satisfies the following properties:*

- (1) $g_{\vartheta,(a)}^{[\eta]}$ belongs to the Sobolev space $W_{\text{loc}}^{1,2}$.
- (2) $g_{\vartheta,(a)}^{[\eta]}$ satisfies the conjugate Beltrami equation (2.36) in $\mathbb{C} \setminus \{a\}$.
- (3) $g_{\vartheta,(a)}^{[\eta]}$ is well defined in simply connected domains of $\mathbb{C} \setminus \{a\}$ and has a monodromy $2i\pi\bar{\eta}$ when winding around a along a positively oriented contour in $\mathbb{C} \setminus \{a\}$.
- (4) $\text{Re}[g_{\vartheta,(a)}^{[\eta]} \cdot \eta]$ is well defined in $\mathbb{C} \setminus \{a\}$ and grows at most logarithmically near a and infinity.

Moreover, the function $g_{\vartheta,(a)}^{[0]}$ is constant.

Let us explain how one can show the existence of this function, combining statements from [5] and [34, Appendix]. We treat the case $a = 0$ and $\eta = 1$ to simplify the reading. Consider $g \in W_{\text{loc}}^{1,2}$ a solution to the conjugate Beltrami equation $\bar{\partial}g = \nu\bar{\partial}g$, where the Beltrami coefficient ν is bounded away from 1. Decompose $g = u + iv$. In that context, one can see from [5, Chapter 16] that u satisfies a *elliptic divergence-form* equation $\text{div}(A_\nu \nabla u) = 0$ where the matrix A_ν is given by [5, Theorem 16.1.6, (16.20)]. Since the Beltrami coefficient is bounded away from 1, the operator A_ν is uniformly elliptic. Moreover, one can reconstruct v by the first order relation $\nabla v = J A_\nu \nabla u$, where J is the Hodge-star operator. The real value function v is the A_ν harmonic conjugate of u (note that it is continuous by standard theory, see e.g. [33]). In the case where the Beltrami coefficient ν is bounded away from 1, this defines uniquely v , up to additive constant. Using again [5, Theorem 16.1.6], in simply connected domains of the complex plane, the function $g = u + iv$ satisfies the conjugate Beltrami equation $\bar{\partial}g = \nu\bar{\partial}g$.

In particular, this allows to use [34, Appendix] and reverse engineer the construction. In the language of that paper, set u to be the fundamental solution for the uniformly elliptic operator $L = A_\nu$, multiplied by 2π given by [34, Theorem A.2]. Note that this function grows logarithmically near 0 and ∞ . Moreover, set v to satisfy $\nabla v = JA_\nu \nabla u$ as above. In that context, $g = u + iv$ indeed satisfies the correct conjugate Beltrami equation. Moreover, g has a monodromy when winding around 0 since \mathbb{C}^* is not simply connected. It is easy to check (see e.g. [46, Lemma 3.3]) that the definition of u coming from [34, Appendix] corresponds to additive monodromy of $2i\pi$ in the present language. Therefore, this constructs a function that indeed satisfies all the wanted properties. The uniqueness statement for this function comes from uniqueness of u in [34, Theorem A.2] and some variant of the Liouville theorem for solutions to conjugate Beltrami equations. In particular, [34, Theorem A.4] ensures the continuity in both variables.

The scaling limit $f_{\vartheta,(a)}^{[\eta]}$ of the full-plane fermions can now be recovered via the Wirtinger derivatives of $g_{\vartheta,(a)}^{[\eta]}$. More precisely, in the ζ -parametrization (2.30), if $f_{\vartheta,(a)}^{[\eta]}$ and $g_{\vartheta,(a)}^{[\eta]}$ are related via (2.35) (and are denoted below by f and g to lighten notation), one has (see [12, Section 2.7])

$$g_\zeta = (\bar{\zeta}f + \zeta\bar{f}\vartheta_z)z_\zeta + \zeta\bar{f}\vartheta_{\bar{z}}\bar{z}_\zeta, \quad (2.38)$$

which allows one to reconstruct $f_{\vartheta,(a)}^{[\eta]}$ from $g_{\vartheta,(a)}^{[\eta]}$, using the facts that $\kappa < 1$, $|\vartheta_z| \leq \frac{\kappa}{2}$, $|\vartheta_{\bar{z}}| \leq \frac{\kappa}{2}$, and $|\bar{z}_\zeta| \leq |\vartheta_\zeta| < |z_\zeta|$. In what follows, we *define* the two-point fermionic full-plane correlator in by setting, for $(a, z) \in \mathbb{C} \times \mathbb{C} \setminus \{(z', z'), z' \in \mathbb{C}\}$,

$$F_\vartheta^{[\eta]}(z, a) := f_{\vartheta,(a)}^{[\eta]}(z) \quad (2.39)$$

We now underline two properties of the functions $F_\vartheta^{[\eta]}$ and comment below on how these properties can be derived rigorously. For any $z_1 \neq z_2$ and any $\eta_1, \eta_2 \in \mathbb{C}$ and $\alpha_1, \alpha_2 \in \mathbb{R}$, one has:

(1) The map $\eta \mapsto F_\vartheta^{[\eta]}(z_1, z_2)$ is real-linear, meaning that

$$F_\vartheta^{[\alpha_1\eta_1 + \alpha_2\eta_2]}(z_1, z_2) = \alpha_1 F_\vartheta^{[\eta_1]}(z_1, z_2) + \alpha_2 F_\vartheta^{[\eta_2]}(z_1, z_2). \quad (2.40)$$

(2) One has the antisymmetrical relation

$$\text{Re}[\bar{\eta}_1 \cdot F_\vartheta^{[\eta_2]}(z_1, z_2)] = -\text{Re}[\bar{\eta}_2 \cdot F_\vartheta^{[\eta_1]}(z_2, z_1)]. \quad (2.41)$$

The proof of the first item can be done via the uniqueness statement of [34, Theorem A.2]. The proof of the second item can be obtained via two different routes. The first route consists in approximating (using [51, Remark 1.3]) the surface (z, ϑ) by an s -embedding of the triangular lattice that satisfies EXP-FAT₀($\delta, \rho(\delta)$) and LIP(κ, δ), proving Theorem 1.2, and using the antisymmetry at the discrete level $\langle \chi_c \chi_a \rangle_{\mathcal{S}^s} = -\langle \chi_a \chi_c \rangle_{\mathcal{S}^s}$. The second possible route is to generalize [16, Lemma 3.15] to the present setup. To lighten notation, set $f_1(z) := F_\vartheta^{[\eta_1]}(z, z_1)$ and $f_2(z) := F_\vartheta^{[\eta_2]}(z, z_2)$. Then the function (see [18, Proposition 2.21])

$$h = \int \text{Im} [f_1(z)f_2(z) dz + f_1(z)\overline{f_2(z)} d\vartheta] \quad (2.42)$$

is well defined away from z_1 and z_2 . Fix a positively oriented circle \mathcal{C}_R of radius R large enough and centered at the midpoint of the segment $[z_1, z_2]$. One can compute the increment of h along \mathcal{C}_R . Reducing the integrals to the sum of two integrals

around small circles centered at z_1 and z_2 and using the respective monodromies, one obtains

$$\int_{\mathcal{C}_R} \operatorname{Im} [f_1(z)f_2(z) dz + f_1(z)\overline{f_2(z)} d\vartheta] = -2\pi \operatorname{Re} [\overline{\eta_1}f_2(z_1) + \overline{\eta_2}f_1(z_2)]. \quad (2.43)$$

Moreover, $f_1(z)$ is uniformly comparable to $(\phi_\vartheta^{[\eta_1]}(\cdot, z_1))_\zeta(z)$, and the latter is $O(R^{-1})$ along \mathcal{C}_R when $R \rightarrow \infty$. A similar observation holds for $f_2(z)$. Sending R to infinity ensures that the integral on the left-hand side of (2.43) vanishes at infinity, yielding the desired identity.

We are now able to define two full-plane basic fermions, following [16, Lemma 3.17], in a way that removes the explicit dependence on η . More precisely, set

$$F_\vartheta(z_1, z_2) := F_\vartheta^{[1]}(z_1, z_2) + iF_\vartheta^{[i]}(z_1, z_2) \quad \text{and} \quad F_\vartheta^*(z_1, z_2) := F_\vartheta^{[1]}(z_1, z_2) - iF_\vartheta^{[i]}(z_1, z_2). \quad (2.44)$$

For any $\eta \in \mathbb{C}$, these satisfy the decomposition

$$F_\vartheta^{[\eta]}(z_1, z_2) = \frac{1}{2}(\overline{\eta}F_\vartheta(z_1, z_2) + \eta F_\vartheta^*(z_1, z_2)). \quad (2.45)$$

When $\vartheta \equiv 0$, it is straightforward to check that $F^{[\eta]}(z, a) = \overline{\eta}[z - a]^{-1}$. Another situation where explicit expressions can be obtained is when the surface (θ, ϑ) is maximal in $\mathbb{R}^{2,1}$. In this case, the parametrization $\zeta \mapsto z(\zeta)$ given in (2.30) is both *conformal and harmonic* (see the discussion in [18, Section 2.5]). In Section 2.6, we parametrize the entire surface $(z, \vartheta(z))_{z \in \mathbb{C}}$ by $\zeta \in \mathbb{C}$, rather than restricting to a bounded subset such as \mathbb{D} . The mapping is proper, meaning that $z(\zeta) \rightarrow \infty$ as $\zeta \rightarrow \infty$. The functions z_ζ , ϑ_ζ , and the Beltrami coefficient ν in (2.36) are all holomorphic in the variable ζ . As will be shown in the proof of Theorem 1.5, this allows one to identify $\phi_{\vartheta, (a)}^{[\eta]}$ (defined via (2.34)) as

$$\phi_{\vartheta, (a)}^{[\eta]}(\zeta) = \frac{c_{a^*}^{[\eta]}}{\zeta - a^*}, \quad (2.46)$$

for some explicit residue $c_{a^*}^{[\eta]}$ (computed in the proof of Theorem 1.5) at the point a^* , corresponding to the preimage of a under the ζ -conformal parametrization. This result provides the explicit formulae on maximal surfaces stated in Theorem 1.3.

3. ONE PRIMITIVE OF THE FULL-PLANE FERMION IS A GREEN FUNCTION

3.1. Constructing the full-plane correlator. We now construct the full-plane energy Kadanoff–Ceva correlator as the limit of the corresponding object in bounded domains. Fix a connected box Λ_R and consider the Ising model on Λ_R with *wired* boundary conditions, meaning that all boundary spins are identified with a single spin attached to the outer face of Λ_R . Fix a corner $a \in \Upsilon$, whose two lifts in Υ^\times are denoted a^+ and a^- . Let $u^\circ(a) \in G^\circ$ and $v^\bullet(a) \in G^\bullet$ be the vertices of $\Lambda(G)$ adjacent to a . Using the formalism introduced in (2.5), with $\varpi = \{u^\circ(a), v^\bullet(a)\}$, we define

$$X_R^{(a)}(c) = \langle \chi_c \chi_a \rangle_{\Lambda_R}^{(w)} := \mathbb{E}^{(w)} [\sigma_{u^\circ(c)} \sigma_{u^\circ(a)} \mu_{v^\bullet(c)} \mu_{v^\bullet(a)}]. \quad (3.1)$$

The correlator $c \mapsto X_R^{(a)}(c)$ is a spinor satisfying the propagation equation (2.6) *everywhere* on $\Upsilon_{(a)}^\times := \Upsilon_{[u^\circ(a), v^\bullet(a)]}^\times$, the double cover that branches everywhere except around $u^\circ(a)$ and $v^\bullet(a)$. As recalled in [17, Figure 6] (see also Figure 4), one can identify the two double covers Υ^\times and $\Upsilon_{(a)}^\times$ except at the corner a , where

the nearby connections to a^\pm are *swapped*. More precisely, the corner $a^+ \in \Upsilon_{(a)}^\times$ is chosen so that the branching structures of $\Upsilon_{(a)}^\times$ and Υ^\times coincide around the quad z_a^+ . In particular, if one required $X_R^{(a)}$ to satisfy the propagation equation everywhere on Υ^\times , one would have to assign $X_R^{(a)}(a^\pm) = \mp 1$ instead of $X_R^{(a)}(a^\pm) = \pm 1$. This observation will play a crucial role in the analysis.

It is standard to construct the full-plane Ising model as a subsequential limit of models defined on an increasing sequence of bounded domains of a weighted planar graph $(S, (x_e)_{e \in E})$. We fix an arbitrary embedding S of $(S, (x_e)_{e \in E})$ into the plane, defined up to homeomorphism. Recall that, in general, for any corner $c \in \Upsilon$, the disorder variable can be written as $\mu_{v^\bullet(c)} \mu_{v^\bullet(a)} = \prod_{e \in \gamma_{(a,c)}^\bullet} x_e^{\varepsilon_e}$, where the product is taken along a disorder line $\gamma_{(a,c)}^\bullet$ connecting a to c , and ε_e denotes the energy density at edge e . Using the identity $x_e^{\varepsilon_e} = \frac{1}{2}[(x_e - x_e^{-1})\varepsilon_e + (x_e + x_e^{-1})]$, one can expand (as in [17, Lemma 4.1]) the *bounded* correlator $X_R^{(a)}$ as

$$X_R^{(a)}(c) = \sum_{\iota \in I(a,c)} a_\iota \mathbb{E}_{\Lambda_R}^{(w)}[\sigma_{A_\iota}], \quad (3.2)$$

where the sum is a finite linear combination of spin correlations, with each product $\sigma_{A_\iota} = \prod_{j \in \iota} \sigma_j$ involving spins along the disorder line $\gamma_{(a,c)}^\bullet$. In particular, the index set $I(a,c)$ does not depend on R (provided R is large enough), and the number of terms remains bounded as $R \rightarrow \infty$. Since $\mathbb{E}_{\Lambda_R}^{(w)}[\sigma_{A_\iota}]$ decreases with R , the quantity $X_R^{(a)}(c)$ admits a well-defined limit $X_S^{(a)}(c)$ as $R \rightarrow \infty$. In the present setting, the strong box-crossing property of Theorem 1.1 holds from some finite scale onward on all s -embeddings considered here. This ensures the existence of a unique full-plane Gibbs measure for all the models involved. Consequently, the limit $X_S^{(a)}(c)$ is independent of the boundary conditions used to define the finite-volume correlators $X_R^{(a)}$. The full-plane correlator $X_S^{(a)}$ thus satisfies the following properties:

- $X_S^{(a)}(a^+) = 1$,
- $X_S^{(a)}$ satisfies the propagation equation (2.6) everywhere in $\Upsilon_{(a)}^\times$.

Keeping the previous identification (except at a) between $\Upsilon_{(a)}^\times$ and Υ^\times , when seen as a function on Υ^\times , the propagation equation around the quad z_a^- fails, while *it would be true if* $X_S^{(a)}(a^\pm) = \mp 1$ instead of the actual fact $X_S^{(a)}(a^\pm) = \pm 1$.

3.2. Identifying one primitive of $X_S^{(a)}$. From now on, we work with a fixed proper s -embedding \mathcal{S}^δ associated with the planar graph S , assuming it satisfies $\text{LIP}(\kappa, \delta)$ and $\text{EXP-FAT}_0(\delta, \rho(\delta))$, with a sufficiently small $\rho(\delta)$. Our goal is to identify one projection of the primitive of $X_S^{(a)}$ as a full-plane Green function on a suitable S-graph associated with \mathcal{S} , at least when δ is small enough. We adopt the following notations, following the formalism developed in Section 2.4.

- For each corner $c \in \Upsilon$, set

$$F_{(a)}^\bullet(c) := (\delta_a \delta_c)^{-\frac{1}{2}} X_S^{(a)}(c) \eta_c.$$

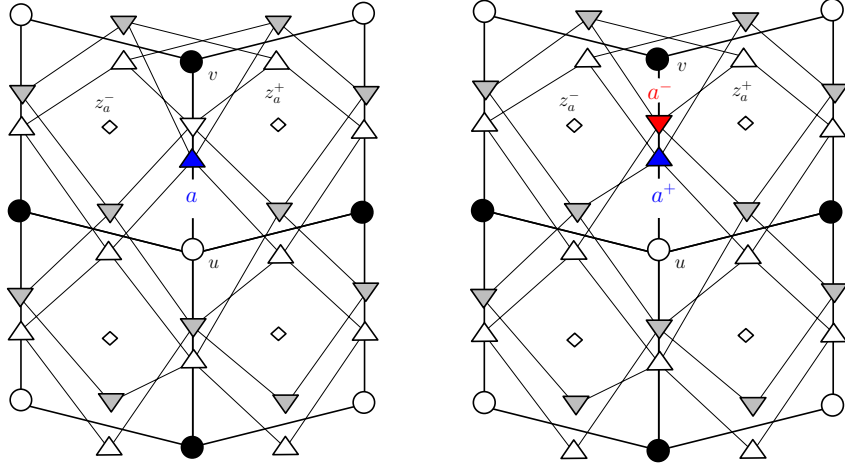


FIGURE 4. (Left) The double cover Υ^x . (Right) The double cover $\Upsilon^x_{(a)}$. The double covers can be identified with each other away from a . The corner a^+ is chosen so that the two double-covers have the same branching structure around the quad z_a^+ . This figure is similar to [17, Figure 6].

The function $\bar{\zeta}F_{(a)}^\bullet$ can be viewed as a t -white holomorphic function (except at the corner a) defined on the black faces $c^\bullet \in B$ of the associated t -embedding. The choice of normalization by $\delta_a^{-1/2}$ will become clear later when computing specific $\Delta^{(\alpha)}$ -Laplacians.

- For each quad $z \in \diamond$, denote by $\bar{\zeta}F_{(a)}^\circ$ the t -white holomorphic function associated with $\bar{\zeta}F_{(a)}^\bullet$ on the white faces $c^\circ \in W$ of the t -embedding (except at $a^\circ \in W$).
- For any quad $z \in \diamond(G)$ and any corner $c \in z$ (except for a), identify c with its adjacent black face $c^\bullet \in B$ and define $F_{(a)}^\circ(z)$ to be the common value taken by $F_{(a)}^\circ$ on one of the white faces $w \in W$ of z . Then

$$F_{(a)}^\bullet(c) = \text{Proj}[F_{(a)}^\circ(z); \eta_c \mathbb{R}].$$

We abbreviate $F_{(a)}^\delta$ for the restriction of $F_{(a)}^\circ$ to \diamond . The functions $F_{(a)}^\delta$ and $X_S^{(a)}(c)$ are related by (2.15).

In what follows, we choose the bipartite coloring of the t -embedding \mathcal{T} attached to \mathcal{S} so that the face a° belongs to the quad z_a^+ . The function $F_{(a)}^\delta$ is s -holomorphic everywhere except at the corner a , where the projections onto $\eta_a \mathbb{R}$ match only up to sign. This is a direct consequence of the same observation made for $X_S^{(a)}$. However, while $F_{(a)}^\delta$ itself is not easy to identify directly, one of its primitives admits a simpler characterization.

The following observation, to the best of our knowledge, remained unnoticed until this paper, even in the square-lattice case. Consider the piecewise differential form (as in (2.16)) defined away from the corner a —that is, in any simply connected

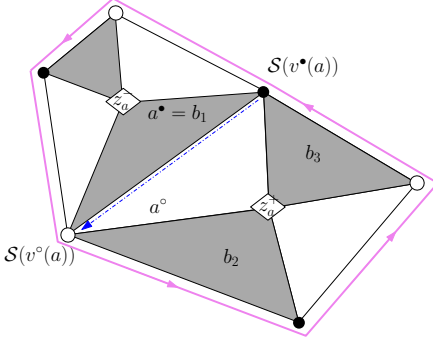


FIGURE 5. Integration trick to identify the full-plane fermion. The contour Γ^δ is shown in pink and can be reduced to an integral over a° . Since $F_{(a)}^\delta$ is not s -holomorphic at a , the mismatch between $\text{Proj}[F_{(a)}^\delta(z_a^+); \eta_a \mathbb{R}]$ and $F_{(a)}^\bullet(a^\bullet) = \text{Proj}[F_{(a)}^\delta(z_a^-); \eta_a \mathbb{R}]$ allows one to compute the residue.

domain not containing a^- by setting

$$I_{(a)}^\delta := \int F_{(a)}^\bullet(c) d\mathcal{S} = \int \bar{\zeta} F_{(a)}^\delta(z) d\mathcal{S} + \varsigma \overline{F_{(a)}^\delta(z)} d\mathcal{Q}. \quad (3.3)$$

This function can be extended to the whole plane in a piecewise-linear fashion together with \mathcal{Q} (see the remark in Section 2.4). We fix the additive normalization of $I_{(a)}^\delta$ so that it vanishes at a point approximating $a + 1$ up to $O(\delta)$ in \mathcal{S}^δ . The differential form $I_{(a)}^\delta$ is well defined in the punctured plane away from a , but it acquires a *monodromy* when winding around a . Using the notation from Figure ??, let Γ^δ be a closed contour (drawn in pink) in the \mathcal{S}^δ plane, oriented positively and winding once around a . Then

$$\int_{\Gamma^\delta} F_{(a)}^\bullet(c) d\mathcal{S} = 2i \bar{\eta}_a. \quad (3.4)$$

Let us now detail this result. First, note that one can deform the pink positively oriented contour Γ^δ and rewrite the integral along Γ^δ as the sum of integrals along two elementary oriented contours, $\Gamma^\delta(z_a^+)$ and $\Gamma^\delta(z_a^-)$, which respectively follow the boundaries of z_a^+ and z_a^- , both oriented positively. The integrals along the four black faces of z_a^+ and z_a^- vanish trivially. Moreover, since the t -holomorphicity relations hold everywhere except at the face a° , the integrals along the white faces of z_a^+ and z_a^- that are distinct from a° also vanish. Hence, the overall integral reduces to the integral along a° , oriented positively.

Recall that the projections of $F_{(a)}^\delta(z_a^+)$ and $F_{(a)}^\delta(z_a^-)$ onto $\eta_a \mathbb{R}$ coincide only *up to sign*. If these projections matched exactly (that is, if $F^\bullet(a^\bullet)$ were replaced by $-F^\bullet(a^\bullet)$), the function $F_{(a)}^\delta$ would be t -holomorphic, and the integral of $F_{(a)}^\bullet$ along a° would vanish. Consequently, the integral along Γ^δ can be rewritten as the mismatch between these projections multiplied by the topological increment (shown in blue) along the segment $[S(v^\circ(a)) - S(v^\bullet(a))]$, yielding the total contribution

$$(\text{Proj}[F_{(a)}^\delta(z_a^-) - F_{(a)}^\delta(z_a^+); \eta_a \mathbb{R}]) \cdot (S(v^\circ(a)) - S(v^\bullet(a))). \quad (3.5)$$

Recalling that $X_S^{(a)}(a^-) = 1$ and $\mathcal{S}^\delta(v^\circ(a)) - \mathcal{S}^\delta(v^\bullet(a)) = i\delta_a \bar{\eta}_a^2$, we obtain the desired result. This, in particular, justifies the normalization by $\delta_a^{-1/2}$, ensuring that the modulus of the monodromy is independent of the lattice scale. We now introduce the real-valued function

$$J_{\mathcal{S}^\delta} := \frac{1}{2} \eta_a \operatorname{Proj}[I_{(a)}^\delta, \bar{\eta}_a \mathbb{R}],$$

which is well defined, as the projection onto $\bar{\eta}_a \mathbb{R}$ removes the monodromy of $I_{(a)}^\delta$. The function $J_{\mathcal{S}^\delta}$ satisfies the following properties:

- (1) Let $\hat{a} := (\mathcal{S}^\delta - i\bar{\eta}_a^2 \mathcal{Q}^\delta)(a^\circ)$ denote the image of the white face $a^\circ \in W$ attached to the corner a in the t -embedding \mathcal{T} . Denote by $b_1, b_2, b_3 \in B$ the three black faces of \mathcal{T} adjacent to $a^\circ \in W$, with $b_1 = a^\bullet$. The vertex \hat{a} is degenerate in $\mathcal{S}^\delta - i\bar{\eta}_a^2 \mathcal{Q}^\delta$. Moreover, for any vertex $v \in \mathcal{S}^\delta - i\bar{\eta}_a^2 \mathcal{Q}^\delta$ such that $v \neq \hat{a}$, one has

$$\Delta^{(\alpha)}[J_{\mathcal{S}^\delta}](v) = 0.$$

This follows from the local closedness of $I_{(a)}^\delta$ away from a , which implies that its projection onto $\bar{\eta}_a \mathbb{R}$ is harmonic in $\mathcal{S}^\delta - i\bar{\eta}_a^2 \mathcal{Q}^\delta$ (see [19, Proposition 4.15] or the computation recalled below).

- (2) At the vertex \hat{a} , one has

$$\Delta^{(\bar{\eta}_a)}[J_{\mathcal{S}^\delta}](\hat{a}) = -\frac{1}{2(S(b_1) + S(b_2) + S(b_3))}.$$

- (3) Provided δ is sufficiently small (but fixed), the function $J_{\mathcal{S}^\delta}$ is sublinear at infinity, meaning that

$$|z|^{-1} \cdot J_{\mathcal{S}^\delta}(z)|_\delta \rightarrow 0 \quad \text{as} \quad |z| \rightarrow \infty,$$

where $|\cdot|_\delta$ denotes the Euclidean distance in the $\mathcal{S}^\delta - i\bar{\eta}_a^2 \mathcal{Q}^\delta$ plane (which is equivalent to the one in the \mathcal{S}^δ plane under $\operatorname{Lip}(\kappa, \delta)$).

Computing the $\Delta^{(\bar{\eta}_a)}$ -Laplacian at \hat{a} is similar to the computation given in [19, Definition 4.12] for a function that is t -holomorphic. We begin by recalling this computation for completeness. Consider a degenerate vertex $\hat{v} = (\mathcal{S}^\delta - i\bar{\eta}_a^2 \mathcal{Q}^\delta)(w)$, corresponding to a white face $w \in W$, and let \hat{F} be a t -white holomorphic function at w . Denote by \hat{F}^\bullet and \hat{F}° the restrictions of \hat{F} to B and W , respectively, and by \hat{I} its associated primitive (in the sense of (2.16)). Finally, for $k = 1, 2, 3$ denote by $\tilde{b}_k \in B$ the faces of \mathcal{T} adjacent to w and \hat{v}_k the endpoint (other than \hat{v}) of the

segment $(\mathcal{S}^\delta - i\bar{\eta}_w^2 \mathcal{Q}^\delta)(\tilde{b}_k)$. Then the harmonicity of $H = I_{\alpha\mathbb{R}}[\tilde{F}]$ for the $\Delta^{(\bar{\eta}_w)}$ -Laplacian reads as

$$\begin{aligned} \sum_{k=1}^3 \frac{m_i}{|\hat{v} - \hat{v}_k|^2} \cdot [H(\hat{v}_i) - H(v)] &= \sum_{k=1}^3 \frac{m_k}{|\hat{v} - \hat{v}_k|^2} \cdot [(\hat{v}_k - \hat{v}) \cdot \hat{F}^\bullet(\tilde{b}_k)] \\ &= \frac{1}{S(\tilde{b}_1) + S(\tilde{b}_2) + S(\tilde{b}_3)} \sum_{k=1}^3 \frac{S(\tilde{b}_k)}{|\hat{v} - \hat{v}_k|^2} \cdot [(\hat{v}_k - \hat{v}) \cdot \hat{F}^\bullet(\tilde{b}_k)] \\ &= \frac{2^{-1}}{S(\tilde{b}_1) + S(\tilde{b}_2) + S(\tilde{b}_3)} \sum_{k=1}^3 |d\mathcal{T}((w\tilde{b}_k)^\star)| \cdot \frac{\hat{v}_k - \hat{v}}{|\hat{v} - \hat{v}_k|} \cdot \hat{F}^\bullet(\tilde{b}_k) \\ &= \frac{2^{-1}}{S(\tilde{b}_1) + S(\tilde{b}_2) + S(\tilde{b}_3)} \sum_{k=1}^3 |d\mathcal{T}((w\tilde{b}_k)^\star)| \cdot (\bar{\eta}_{b_k} \cdot \bar{\varsigma} \cdot \bar{\eta}_w) \cdot \hat{F}^\bullet(\tilde{b}_k) \\ &= \frac{2^{-1}\bar{\varsigma} \cdot \bar{\eta}_w}{S(\tilde{b}_1) + S(\tilde{b}_2) + S(\tilde{b}_3)} \cdot \eta_w \sum_{k=1}^3 d\mathcal{T}((w\tilde{b}_k)^\star) \cdot \hat{F}^\bullet(\tilde{b}_k) = 0. \end{aligned}$$

Here, the first equality defines the $\Delta^{(\bar{\eta}_w)}$ -Laplacian; the second uses the explicit coefficients m_k ; the third applies the identity $S(\tilde{b}_k) = \frac{1}{2}|\hat{v} - \hat{v}_k||d\mathcal{T}((w\tilde{b}_k)^\star)|$ from [19, Fig. 7(right)]; the fourth uses $\hat{v}_k - \hat{v} = \bar{\eta}_{b_k} \bar{\varsigma} \bar{\eta}_w |\hat{v} - \hat{v}_k|$; the fifth follows from $\bar{\eta}_{b_k} |d\mathcal{T}((w\tilde{b}_k)^\star)| = \eta_w d\mathcal{T}((w\tilde{b}_k)^\star)$ (see [19, Def. 2.4]); and the last equality follows from the vanishing contour integral $\sum_{k=1}^3 d\mathcal{T}((w\tilde{b}_k)^\star) \hat{F}^\bullet(\tilde{b}_k) = 0$ for t -holomorphic functions.

Recalling the above computation, one can now deduce $\Delta^{(\bar{\eta}_a)}[J_{\mathcal{S}^\delta}](\hat{a})$. Indeed, applying the same strategy to $\hat{F} = \bar{\varsigma} F_{(a)}^\bullet$ around the white face of the t -embedding $w = a^\circ$, collapsed to \hat{a} , yields the result. As in the monodromy computation, if one had $\bar{\varsigma} F_{(a)}^\bullet(a^\bullet) = -\bar{\eta}_a \delta_a^{-1}$ instead of the actual value $\bar{\varsigma} F_{(a)}^\bullet(a^\bullet) = \bar{\eta}_a \delta_a^{-1}$, the projections of $\bar{\varsigma} F_{(a)}^\circ(z_{(a)}^\pm)$ on $\eta_{a^\bullet} \mathbb{R}$ would coincide, making $J_{\mathcal{S}^\delta}$ harmonic at \hat{a} . Reinjecting this observation into the above computation, one readily obtains

$$\sum_{k=1}^3 d\mathcal{T}((w\tilde{b}_k)^\star) \cdot \bar{\varsigma} F_{(a)}^\bullet(b_k) = 2 \times (\bar{\varsigma} F_{(a)}^\bullet(a^\bullet)) \times d\mathcal{T}((a^\circ a^\bullet)^\star) = 2\bar{\eta}_a \delta_a^{-1} \cdot i\delta_a \bar{\eta}_a^{-2}, \quad (3.6)$$

$d\mathcal{T}((a^\circ a^\bullet)^\star) = \mathcal{S}^\delta(v^\circ(a)) - \mathcal{S}^\delta(v^\bullet(a))$ (when winding in the positive direction around the white face a° the increment along the segment separating a^\bullet and a° is oriented from $\mathcal{S}^\delta(v^\bullet(a))$ towards $\mathcal{S}^\delta(v^\circ(a))$). This allows to conclude.

We now prove sublinearity at infinity, still assuming $\text{LIP}(\kappa, \delta)$ and $\text{EXP-FAT}_0(\delta, \rho(\delta))$. The first step is to compare the values of $|F_{(a)}^\bullet|$ and $|F_{(a)}^\circ|$ in a given region. According to [19, Lemma 6.21], under $\text{LIP}(\kappa, \delta)$ there exist constants $\gamma_0(\kappa), C_0(\kappa) > 0$, depending only on κ , such that whenever $\frac{1}{4} \leq 4R \leq |u - a|$, the following alternative holds:

- (A) $\max_{z \in B(u, \frac{R}{2})} |F_{(a)}^\circ(z)| \leq C_0(\kappa) \max_{c \in B(u, R)} |F_{(a)}^\bullet(c)|,$
- (B) $\max_{z \in B(u, \frac{3}{4}R)} |F_{(a)}^\circ(z)| \geq C_0(\kappa) \exp(\gamma_0(\kappa)R\delta^{-1}) \max_{c \in B(u, R)} |F_{(a)}^\bullet(c)|.$

Under the assumption $\text{EXP-FAT}_0(\delta, \rho(\delta))$, we show that scenario (B) cannot occur in the limit $\delta \rightarrow 0$, provided we stay at a fixed distance from a . Indeed, for sufficiently small δ , there exists at least one circuit Γ^δ in the annulus $A(u, 0.8R, 0.9R)$ composed of $D(\delta)$ -fat faces, where $D(\delta) := \delta \exp[-\rho(\delta)\delta^{-1}]$. For any $z \in \Gamma^\delta$, the reconstruction formula of [19, Cor. 6.18] gives

$$|F_{(a)}^\circ(z)| \leq 2D(\delta)^{-1} \max_{c \in \Gamma^\delta} |F_{(a)}^\bullet(c)|.$$

Moreover, following the proof of [19, Cor. 6.18], one may replace the ball $B(u, R)$ in the alternative (B) by the interior of Γ^δ , adjusting the constant $\gamma_0(\kappa) > 0$ if necessary. Since $z \mapsto |F_{(a)}^\circ(z)|$ satisfies the discrete maximum principle (see [12, Rem. 2.9]), this alternative (B) would imply that

$$\begin{aligned} 2\delta^{-1} \cdot \exp(\rho(\delta) \cdot \delta^{-1}) \cdot \max_{c \in \Gamma^\delta} |F_{(a)}^\bullet(c)| &\geq \max_{z \in \Gamma^\delta} |F_{(a)}^\circ(z)| \\ &\geq \max_{z \in B(u, \frac{3}{4}R)} |F_{(a)}^\circ(z)| \\ &\geq C_0(\kappa) \exp(\gamma_0(\kappa)R\delta^{-1}) \max_{c \in B(u, R)} |F_{(a)}^\bullet(c)|, \end{aligned}$$

which is impossible in the $\delta \rightarrow 0$ regime as $R \geq \frac{1}{4}$.

We now conclude the proof of sublinearity for $J_{\mathcal{S}^\delta}$. By the standard Kadanoff-Ceva formalism and the strong box-crossing property, for sufficiently small δ and $|\mathcal{S}^\delta(a) - \mathcal{S}^\delta(c)| \geq \frac{1}{4}$ one has for any corner c

$$|\langle \chi_c \chi_a \rangle_{\mathcal{S}^\delta}| \leq \mathbb{E}_{\mathcal{S}^\delta} [\mu_{v^\bullet(a)} \mu_{v^\bullet(c)}] \leq O\left(\left[\frac{\rho(\delta)}{|\mathcal{S}^\delta(a) - \mathcal{S}^\delta(c)|}\right]^{\beta(\kappa)}\right) \rightarrow 0, \quad (3.7)$$

as $|\mathcal{S}^\delta(a) - \mathcal{S}^\delta(c)|_\delta \rightarrow \infty$, where O and $\beta(\kappa)$ depend only on κ .

For a *fixed* grid \mathcal{S}^δ with δ small, the quantity $(\delta_a D(\delta))^{-1}$ is a uniform lattice-dependent constant. Combined with (3.7), this implies that on $D(\delta)$ -fat quads, $|F_{(a)}^\bullet(c)| \rightarrow 0$ uniformly as $c \rightarrow \infty$. By the reconstruction formula [19, Cor. 6.18], the same holds for $|F_{(a)}^\circ(z)|$, which thus vanishes uniformly at infinity on $D(\delta)$ -fat quads. Applying the discrete maximum principle to $z \mapsto |F_{(a)}^\circ(z)|$ then yields

$$|F_{(a)}^\circ(z)| \rightarrow 0 \text{ as } |\mathcal{S}^\delta(a) - \mathcal{S}^\delta(z)|_\delta \rightarrow \infty.$$

Integrating from $a + 1$ (where $I_{(a)}^\delta$ vanishes) shows that $I_{(a)}^\delta$ is sublinear at infinity. Since distances in \mathcal{S}^δ and $\mathcal{S}^\delta - i\bar{\eta}_a^2 \mathcal{Q}^\delta$ are comparable up to a uniform κ -dependent factor, $J_{\mathcal{S}^\delta}$ is also sublinear at infinity. This argument implicitly uses the uniform existence of $D(\delta)$ -fat circuits across the plane, which holds under $\text{EXP-FAT}_0(\delta, \rho(\delta))$.

3.3. Construction of full-plane Green kernel. We saw in the previous subsection that one can interpret one projection of the primitive of the infinite-volume fermionic correlation as a solution to a full-plane boundary value problem. It is thus natural to reformulate this as a full-plane Green function, since we are seeking a function that is harmonic almost everywhere, has a prescribed $\Delta^{(\alpha)}$ -Laplacian at the vertex where harmonicity fails, and is sub-linear at infinity.

The goal of this section is to make this identification rigorous. We begin by explicitly constructing a full-plane Green function on a given S-graph (as a regularisation of its finite-volume counterparts), and then identify it with $J_{\mathcal{S}^\delta}$. Under the assumption $\text{LIP}(\kappa, \delta)$, it is straightforward to verify that random walks on S-graphs

are recurrent, making the construction of a full-plane Green function non-trivial. The key estimates required to pass from the (regularised) Green function in bounded domains to its infinite-volume limit are given by Proposition 3.1, obtained by Basok in [6, Proposition 3.1], following ideas already present in [18, Theorem 3.1].

From now on, we work on a fixed s -embedding \mathcal{S}^δ satisfying $\text{LIP}(\kappa, \delta)$ for some fixed $\kappa < 1$ and mesh size δ . In what follows, $D(a, P)$ denotes an $O(\delta)$ -approximation of the Euclidean disc of radius P centred at a . In particular, all estimates below are uniform in $\kappa < 1$. Working on the S-graph $\mathcal{S}^\delta + \lambda^2 \mathcal{Q}^\delta$ and assuming P is sufficiently large, define for $a, b \in \mathcal{S}^\delta + \lambda^2 \mathcal{Q}^\delta$

$$G_P^{(\lambda)}(a, b) := \mathbb{E}_b [\text{time spent at } a \text{ before leaving } D(a, P)], \quad (3.8)$$

where the expectation is taken with respect to the directed random walk $X^{(\lambda)}$ of Definition 2.9, started at b . The corresponding invariant measure $\mu = \mu^{(\lambda)}$ admits a geometric interpretation in \mathcal{S}^δ , as recalled in Section 2.4.

We now introduce a regularised and rescaled version of $G_P^{(\lambda)}$, whose continuous analogue admits a non-trivial limit as $\delta \rightarrow 0$ and $P \rightarrow \infty$ (we omit the δ, λ indices for readability):

$$M_P(b) := \frac{G_P^{(\lambda)}(a, b) - G_P^{(\lambda)}(a, a+1)}{\mu^{(\lambda)}(a)}. \quad (3.9)$$

The following proposition controls the oscillations of M_P , with bounds depending only on κ .

Proposition 3.1 (Proposition 3.1 in [6]). *Assume that the vertex a is degenerate in $\mathcal{S}^\delta + \lambda^2 \mathcal{Q}^\delta$. Then there exist κ -dependent constants $C_{0,1}(\kappa)$, uniform in P , such that for any $b, b' \in \mathcal{S}^\delta + \lambda^2 \mathcal{Q}^\delta$ satisfying the following condition denoted (\star)*

$$C_0(\kappa)\rho(\delta) \leq |b - a|_\delta; \quad 2^{-1} \leq |b - a|_\delta |b' - a|_\delta^{-1} \leq 2, \quad \max(100|b - a|_\delta, 2) \leq P,$$

one has the oscillation estimate

$$|M_P(b) - M_P(b')| \leq C_1(\kappa). \quad (3.10)$$

In the above, the distance $|\cdot|_\delta$ denotes that in the $\mathcal{S}^\delta + \lambda^2 \mathcal{Q}^\delta$ -plane, which is uniformly comparable (starting from some scale $O(\delta)$), only depending on κ , to the Euclidean distance in the \mathcal{S}^δ .

The additive and multiplicative scaling factors in (3.9) are chosen to yield a non-trivial object in the limit $\delta \rightarrow 0$, exhibiting logarithmic growth near a . Basok's proof proceeds by contradiction, assuming the oscillations of the Green function are not uniformly bounded across a sequence of annuli, he extracts a subsequence that violates the expected continuous behaviour (using the Sloïlov factorisation) by oscillating too rapidly compared to its continuous analogue.

We are now ready to construct the full-plane Green kernel on $\mathcal{S}^\delta + \lambda^2 \mathcal{Q}^\delta$, following [6, Section 3]. Its gradient is an s -holomorphic function everywhere on \mathcal{S}^δ except at one corner, where the projections in (2.13) fail to match.

Proposition 3.2. *Let the S-graph $\mathcal{S}^\delta + \lambda^2 \mathcal{Q}^\delta$ be degenerate at a . Then, provided δ is sufficiently small, there exists a unique real-valued function $M_\infty^{(\lambda)}$ on $\mathcal{S}^\delta + \lambda^2 \mathcal{Q}^\delta$ such that:*

- (1) *For all $v \neq a$, $\Delta^{(\lambda)}[M_\infty^{(\lambda)}](v) = 0$.*
- (2) *At the degenerate vertex a , one has $\Delta^{(\lambda)}[M_\infty^{(\lambda)}](a) = \mu^{(\lambda)}(a)^{-1}$.*

(3) $M_\infty^{(\lambda)}(a+1) = 0$.
 (4) $M_\infty^{(\lambda)}$ is sub-linear at infinity on $\mathcal{S}^\delta + \lambda^2 \mathcal{Q}^\delta$, i.e.

$$\lim_{|z|_\delta \rightarrow \infty} |z|_\delta^{-1} |M_\infty^{(\lambda)}(z)| = 0.$$

As a consequence of the construction in the proof, there exist constants $C_{0,1}(\kappa)$ such that for any $b, b' \in \mathcal{S}^\delta + \lambda^2 \mathcal{Q}^\delta$ satisfying the condition (4) one has

$$|M_\infty(b) - M_\infty(b')| \leq C_1(\kappa). \quad (3.11)$$

This allows us to identify

$$J_{\mathcal{S}^\delta} = -\frac{1}{2} M_\infty^{\overline{\zeta \eta_a}},$$

where the function $J_{\mathcal{S}^\delta}$ is the one constructed in Section 3.1.

Proof. Uniqueness. We first show that only one function can satisfy (1)-(4). Let M^1 and M^2 be two such functions and set $M = M^1 - M^2$. Then M is harmonic everywhere on $\mathcal{S}^\delta + \lambda^2 \mathcal{Q}^\delta$, and its gradient F (see [19, Def. 4.12]) is s -holomorphic on \mathcal{S}^δ . Fix a ball of radius R in \mathcal{S}^δ , centered at $a^\circ \in \mathcal{S}^\delta$, corresponding to the preimage of the degenerate vertex $a \in \mathcal{S}^\delta + \lambda^2 \mathcal{Q}^\delta$. By the Harnack inequality (Theorem 2.1 in the EXP-FAT₀($\delta, \rho(\delta)$) in the regime $\delta \rightarrow 0$), there exists $C(\kappa) > 0$ such that

$$\max_{B(a^\circ, R)} |F| \leq C(\kappa) \frac{\text{osc}_{B(a^\circ, 2R)} M}{R}. \quad (3.12)$$

Since M is sublinear at infinity, letting $R \rightarrow \infty$ yields $F \equiv 0$. Hence M is constant, and property (3) completes the uniqueness proof.

Existence. We now establish existence, building on Proposition 3.1. Recall that the map $b \mapsto M_P(b)$ is harmonic for the random walk on $\mathcal{S}^\delta + \lambda^2 \mathcal{Q}^\delta$ except at a , i.e. $\Delta^{(\lambda)}[M_P^{(\lambda)}](v) = 0$ for $v \neq a$. The construction proceeds in two steps.

Step 1: Away from a . For $C_0(\kappa)$ as in Proposition 3.1 and any $R \geq C_0 \rho(\delta)$, the oscillations $\text{osc}_{A(a, R, 2R)} M_P^{(\lambda)}$ in the annulus $A(a, R, 2R) \subset \mathcal{S}^\delta + \lambda^2 \mathcal{Q}^\delta$ are uniformly bounded for large enough P . Since each $M_P^{(\lambda)}$ vanishes at $a+1$, the family $(M_P^{(\lambda)})_{P \geq 2}$ is uniformly bounded on compacts of $\mathcal{S}^\delta + \lambda^2 \mathcal{Q}^\delta$ lying at least $C_0 \rho(\delta)$ away from a . A diagonal extraction as $P \rightarrow \infty$ yields a limit function $M_\infty^{(\lambda)}$, harmonic on $(\mathcal{S}^\delta + \lambda^2 \mathcal{Q}^\delta) \setminus D(a, C_0 \rho(\delta))$, vanishing at $a+1$, and satisfying the oscillation bounds of Proposition 3.1.

Step 2: Extension near a . Extend $M_\infty^{(\lambda)}$ inside $D(a, C_0 \rho(\delta))$ by

$$M_\infty^{(\lambda)}(b) := \frac{G_{\mathcal{C}^\delta}^{(\lambda)}(b, a)}{\mu^{(\lambda)}(a)} + H_{\mathcal{C}^\delta}, \quad (3.13)$$

where $G_{\mathcal{C}^\delta}^{(\lambda)}$ is the Green function of $\Delta^{(\lambda)}$ on $D(a, C_0 \rho(\delta))$ with boundary values matching those of $M_\infty^{(\lambda)}$.

Away from the preimage of a in \mathcal{S}^δ , the gradient F_∞^δ of $M_\infty^{(\lambda)}$ is s -holomorphic. Under $\text{LIP}(\kappa, \delta)$ and EXP-FAT₀($\delta, \rho(\delta)$), the second case of Theorem 2.1 applies, giving $C(\kappa) > 0$ such that for $|\mathcal{S}^\delta(a^\circ) - \mathcal{S}^\delta(z)| \geq C_2(\kappa) \rho(\delta)$,

$$|F_\infty^\delta(z)| \leq \frac{C(\kappa)}{|\mathcal{S}^\delta(a) - \mathcal{S}^\delta(z)|} \text{osc}_{B(z, \frac{1}{2} |\mathcal{S}^\delta(a^\circ) - \mathcal{S}^\delta(z)|)} M_\infty^{(\lambda)}. \quad (3.14)$$

Since the oscillations of $M_\infty^{(\lambda)}$ are uniformly bounded away from a° , there exists a constant $O(1)$ depending only on κ such that, for δ small,

$$|F_\infty^\delta(z)| = \frac{O(1)}{|\mathcal{S}^\delta(a) - \mathcal{S}^\delta(z)|}. \quad (3.15)$$

Integrating (3.15) from $a + 1$ to infinity shows that $M_\infty^{(\lambda)}$ is sublinear at infinity, establishing property (4).

To complete the proof, we compute $\Delta^{(\lambda)}[M_\infty^{(\lambda)}](a)$. Recall that the random walk $X^{(\lambda)}$ jumps from a vertex v to a neighbour v_k after an exponential time τ_v with parameter $t_v = \sum_{v_k \sim v} q^{(\lambda)}(v_k)$. Starting from a (adjacent to v_1, v_2, v_3), the Markov property gives

$$G_P(a, a) = \mathbb{E}[\tau_v] + \sum_{k=1}^3 \frac{q^{(\lambda)}(a \rightarrow v_k)}{\sum_{j=1}^3 q^{(\lambda)}(a \rightarrow v_j)} G_P(a, v_k). \quad (3.16)$$

Since $\mathbb{E}[\tau_v] = (t_v)^{-1}$, we obtain $\Delta^{(\lambda)}[M_\infty^{(\lambda)}](a) = \mu^{(\lambda)}(a)^{-1}$. The same holds in the limit $P \rightarrow \infty$, completing the construction. Finally, one can use the uniqueness statement to identify $J_{\mathcal{S}^\delta} = -\frac{1}{2} M_\infty^{(\lambda)} \eta_a$, using the interpretation of $\mu^{(\lambda)}$ made in Section 2.4 in terms of black triangles areas. \square

4. PROOFS OF CONVERGENCE STATEMENTS

In this section, we identify the n -point fermionic correlators with their continuous counterparts. Since multipoint correlators of the form $\langle \chi_{a_1} \dots \chi_{a_n} \rangle_{\mathcal{S}^\delta}$ satisfy a Pfaffian structure (see, e.g., [16, Proposition 2.24]), it suffices to establish the convergence of the two-point fermions $\langle \chi_c \chi_a \rangle_{\mathcal{S}^\delta}$ in order to recover the full scaling limit of $\langle \chi_{a_1} \dots \chi_{a_n} \rangle_{\mathcal{S}^\delta}$. Their corresponding continuous object now involves the generalisation of the classical logarithm discussed in Section 2.7, where the holomorphy condition is replaced by the conjugate Beltrami equation (2.36). We are now ready to prove Theorem 1.2.

Let $F_{(a^\delta)}$ denote the complexified s -holomorphic function associated with the fermionic correlator $c \mapsto (\delta_a)^{-\frac{1}{2}} \langle \chi_c \chi_{a^\delta} \rangle_{\mathcal{S}^\delta}$. A key difficulty in the proof lies in ensuring that the family $(F_{(a^\delta)})_{\delta > 0}$ is indeed precompact away from a and therefore admits a non-trivial continuous limit. This is precisely where identifying one primitive of $F_{(a^\delta)}$ with a suitable Green function provides additional information through its random walk interpretation and determines the correct scaling factor. In particular, this shows that the exact scaling factor of the *combinatorial fermion* $\langle \chi_c \chi_{a^\delta} \rangle_{\mathcal{S}^\delta}$ is local, fully explicit, and given by $(\delta_a^\delta \delta_c^\delta)^{-\frac{1}{2}}$.

Proof of Theorem 1.2. Fix a sequence $\delta_k \rightarrow 0$ (we drop the subscript k from now on) and continue to denote $J_{\mathcal{S}^\delta} := \frac{1}{2} \eta_{a^\delta} \text{Proj}[I_{(a^\delta)}, \bar{\eta}_{a^\delta} \mathbb{R}]$, where $I_{(a^\delta)}$ is defined as in (3.3) and vanishes near $a^\delta + 1$. According to Proposition 3.2, one deduces that, provided δ is sufficiently small, $J_{\mathcal{S}^\delta} = -\frac{1}{2} M_\infty^{(\lambda)} \eta_a$. Since the oscillations of $M_\infty^{(\lambda)}$ are uniformly bounded in macroscopic annuli of $\mathbb{C} \setminus \{a\}$, it follows, as in the proof of Proposition 3.2, that $|F_{(a^\delta)}(z)| = O(|\mathcal{S}^\delta(z) - \mathcal{S}^\delta(a^\delta)|^{-1})$, where the implied constant depends only on κ .

In particular, the functions $(F_{(a^\delta)})_{\delta > 0}$ are uniformly bounded on compacts of $\mathbb{C} \setminus \{a\}$, allowing one to extract subsequential limits by Remark 2.10. Thus, there

exists a subsequence $\delta \rightarrow 0$ such that

$$F_{(a^\delta)} \xrightarrow[\delta \rightarrow 0]{} f_a \quad \text{uniformly on compacts of } \mathbb{C} \setminus \{a\}. \quad (4.1)$$

Up to passing to another subsequence, one may also assume that $\eta_{a^\delta} \rightarrow \eta_a \in \mathbb{T}$. Following Section 2.6, on simply connected domains of $\mathbb{C} \setminus \{a\}$, the differential form $\bar{\zeta} f_a dz + \zeta \bar{f}_a d\vartheta$ is closed, while f_a remains uniformly bounded (indeed, we already know that at discrete level $|F_{(a^\delta)}(z)| = O(|\mathcal{S}^\delta(z) - \mathcal{S}^\delta(a^\delta)|^{-1})$). In the ζ quasiconformal parametrization introduced in Section 2.6, the primitive $g_a(\zeta) := I_{\mathbb{C}}[f_a]$ defined by (2.35) satisfies the following properties:

- g_a satisfies the conjugate Beltrami equation (2.36) and belongs to $W_{\text{loc}}^{(1,2)}$, since f_a is uniformly bounded on compacts of $\mathbb{C} \setminus \{a\}$.
- $\text{Re}[\eta_a g_a]$ is well defined in $\mathbb{C} \setminus \{a\}$ and grows at most logarithmically near a and at infinity. Indeed, the discrete estimates $|F_{(a^\delta)}(z)| = O(|\mathcal{S}^\delta(z) - \mathcal{S}^\delta(a^\delta)|^{-1})$ directly imply that $f_a(z) = O(|z - a|^{-1})$. Integrating this bound from $a + 1$ yields the claim.
- g_a has a monodromy $2i\bar{\eta}_a$ when winding once around a simple positively oriented loop enclosing a . To see this, take a smooth positively oriented loop γ encircling a and discretize it in \mathcal{S}^δ by γ^δ . The contour γ^δ can be deformed into an elementary contour of \mathcal{S}^δ containing the two quads $z_{a^\delta}^+$ and $z_{a^\delta}^-$. Repeating the computation in (3.4) shows that the integral over γ^δ equals $2i\bar{\eta}_{a^\delta}$. Passing to the limit $\delta \rightarrow 0$ (for γ^δ , which stays away from a) yields that the monodromy of g_a along γ is $2i\bar{\eta}_a$.

This identifies g_a as the function $\pi^{-1} \cdot g_{\vartheta,(a)}^{[\eta_a]}$ introduced in Section 2.7. Consequently, f_a converges to $\pi^{-1} \cdot f_{\vartheta,(a)}^{[\eta_a]}$ uniformly on compacts of $\mathbb{C} \setminus \{a\}$. Projecting over the edge containing c^δ concludes the proof. \square

We are now in a position to extend the previous convergence result to multipoint Kadanoff–Ceva correlators, using the Pfaffian structure of Ising fermions. Let us recall a standard definition from linear algebra. Given a $2n \times 2n$ antisymmetric matrix $A = (a_{ij})_{1 \leq i,j \leq 2n}$, its Pfaffian **Pfaff** is defined by

$$\mathbf{Pfaff}[A] := \frac{1}{2^n n!} \sum_{\sigma \in \mathcal{S}_n} \text{sgn}(\sigma) \prod_{k=1}^n a_{\sigma(2k), \sigma(2k+1)}. \quad (4.2)$$

The Pfaffian structure of Ising fermions then yields the convergence of all $2n$ -point correlators. This is stated in the following theorem.

Theorem 4.1. *Fix $2n$ corners $p_1^\delta, \dots, p_{2n}^\delta \in \mathcal{S}^\delta$ approximating respectively the pairwise distinct points $p_1, \dots, p_{2n} \in \mathbb{C}$. Then one has*

$$\left(\prod_{k=1}^{2n} \delta_{p_k^\delta} \right)^{-\frac{1}{2}} \langle \chi_{p_1^\delta} \chi_{p_2^\delta} \cdots \chi_{p_{2n}^\delta} \rangle_{\mathcal{S}^\delta} = \frac{1}{\pi^n} \mathbf{Pffaf} \left[\text{Re}[\bar{\eta}_{p_i^\delta} \cdot F_{\vartheta}^{[n_{p_j^\delta}]}(p_j, p_i)] \right]_{j,k=1}^{2n} + o_{\delta \rightarrow 0}(1), \quad (4.3)$$

where $o_{\delta \rightarrow 0}(1)$ is uniform in $\kappa < 1$ and on compacts of $\mathbb{C} \setminus \{p_1, \dots, p_{2n}\}$.

Proof. The proof follows directly once Theorem 1.2 has been established. Indeed, even before passing to the limit, one can apply the Pfaffian identity for Kadanoff–Ceva correlators (see, e.g., [16, Proposition 2.24] or [4, Theorem 6.1]). After a

suitable identification of the corresponding double covers, this gives

$$\langle \chi_{p_1^\delta} \chi_{p_2^\delta} \cdots \chi_{p_{2n}^\delta} \rangle_{\mathcal{S}^\delta} = \mathbf{Pfaff} [\langle \chi_{p_i^\delta} \chi_{p_j^\delta} \rangle_{\mathcal{S}^\delta}]_{i,j=1}^{2n}. \quad (4.4)$$

One can then let $\delta \rightarrow 0$ and use the convergence of the two-point correlators from Theorem 1.2 to conclude. \square

We are now ready to conclude and prove Theorem 1.3, with a minor refinement in the analysis. Indeed, the full-plane energy density random variable arises as a particular value of the Kadanoff–Ceva fermion $\langle \chi_{(\cdot)} \chi_{a^\delta} \rangle_{\mathcal{S}^\delta}$ in the vicinity of a^δ . More precisely, assume that the corners a^δ and b^δ are neighboring within the quad z_{e^δ} , sharing the same primal vertex $v^\bullet(a^\delta) = v^\bullet(b^\delta)$. It is straightforward to verify that $\langle \chi_{b^\delta} \chi_{a^\delta} \rangle_{\mathcal{S}^\delta} = \mathbb{E}_{\mathcal{S}^\delta} [\varepsilon_{e^\delta}]$. Consequently, to obtain the convergence stated in Theorem 1.3, one must *fuse* the corners pairwise (that is, $p_{2k} = p_{2k+1}$ in the previous formalism). The proof below explains this refinement, which allows us to recover the scaling limit of the full-plane energy density.

Proof of Theorem 1.3. Fix two distinct points $p_1 \neq p_2$ in the complex plane, approximated respectively by $z_{e_1^\delta}$ and $z_{e_2^\delta}$. Consider two pairs of corners $a_1^\delta, b_1^\delta \in z_{e_1^\delta}$ and $a_2^\delta, b_2^\delta \in z_{e_2^\delta}$, each pair sharing the same primal vertex, that is $v^\bullet(a_1^\delta) = v^\bullet(b_1^\delta)$ and $v^\bullet(a_2^\delta) = v^\bullet(b_2^\delta)$. It is straightforward to verify that

$$\langle (\chi_{b_1^\delta} \chi_{a_1^\delta} - \langle \chi_{b_1^\delta} \chi_{a_1^\delta} \rangle_{\mathcal{S}^\delta}) \cdot (\chi_{b_2^\delta} \chi_{a_2^\delta} - \langle \chi_{b_2^\delta} \chi_{a_2^\delta} \rangle_{\mathcal{S}^\delta}) \rangle_{\mathcal{S}^\delta} = \mathbb{E}_{\mathcal{S}^\delta} [(\varepsilon_{e_1^\delta} - \mathbb{E}_{\mathcal{S}^\delta} [\varepsilon_{e_1^\delta}]) \cdot (\varepsilon_{e_2^\delta} - \mathbb{E}_{\mathcal{S}^\delta} [\varepsilon_{e_2^\delta}])].$$

We can now expand the correlator $\langle \chi_{b_1^\delta} \chi_{a_1^\delta} \chi_{b_2^\delta} \chi_{a_2^\delta} \rangle_{\mathcal{S}^\delta}$ using the Pfaffian structure of Ising fermions, which gives

$$\mathbb{E}_{\mathcal{S}^\delta} [(\varepsilon_{e_1^\delta} - \mathbb{E}_{\mathcal{S}^\delta} [\varepsilon_{e_1^\delta}]) \cdot (\varepsilon_{e_2^\delta} - \mathbb{E}_{\mathcal{S}^\delta} [\varepsilon_{e_2^\delta}])] = -\langle \chi_{b_1^\delta} \chi_{b_2^\delta} \rangle_{\mathcal{S}^\delta} \langle \chi_{a_1^\delta} \chi_{a_2^\delta} \rangle_{\mathcal{S}^\delta} + \langle \chi_{a_1^\delta} \chi_{b_2^\delta} \rangle_{\mathcal{S}^\delta} \langle \chi_{b_1^\delta} \chi_{a_2^\delta} \rangle_{\mathcal{S}^\delta}.$$

Dividing both sides by $(\delta_{a_1^\delta} \delta_{b_1^\delta} \delta_{a_2^\delta} \delta_{b_2^\delta})^{1/2}$ and using the convergence of the two-point fermionic correlators from Theorem 1.2, we obtain that the (rescaled) left-hand side of the above equation converges to

$$-\pi^{-2} \left(\operatorname{Re} [\bar{\eta}_{b_1^\delta} \cdot f_\vartheta^{[\eta_{b_2^\delta}]} (p_1, p_2)] \operatorname{Re} [\bar{\eta}_{a_1^\delta} \cdot f_\vartheta^{[\eta_{a_2^\delta}]} (p_1, p_2)] \right. \\ \left. + \operatorname{Re} [\bar{\eta}_{a_1^\delta} \cdot f_\vartheta^{[\eta_{b_2^\delta}]} (p_1, p_2)] \operatorname{Re} [\bar{\eta}_{b_1^\delta} \cdot f_\vartheta^{[\eta_{a_2^\delta}]} (p_1, p_2)] \right).$$

Expanding the functions $f_\vartheta^{[\eta]}$ in the basis $(F_\vartheta, F_\vartheta^*)$, rewrites the above as

$$-\pi^{-2} \frac{1}{4} \operatorname{Im} [\bar{\eta}_{a_1^\delta} \eta_{b_1^\delta}] \operatorname{Im} [\bar{\eta}_{a_2^\delta} \eta_{b_2^\delta}] (|F_\vartheta(p_1, p_2)|^2 - |F_\vartheta^*(p_1, p_2)|^2).$$

Finally, using the formulae of (2.9) one sees that $r_{e_1^\delta} = -\cos(\theta_{e_1^\delta}) \operatorname{Im} [\bar{\eta}_{a_1^\delta} \eta_{b_1^\delta}] (\delta_{a_1^\delta} \delta_{b_1^\delta})^{1/2}$ and similarly for the edge e_2^δ , which allows to conclude the proof.

Let us now prove give explicit formulae when the surface (z, ϑ) is maximal in $\mathbb{R}^{(2,1)}$. Let p_1^*, p_2^* be the pre-images of $p_{1,2}$ in the *full-plane* ζ parametrisation (2.31). It will be detailed inside the proof of Theorem 1.5 that one has (4.14) (with a multiplicative difference of π^{-1} factors as residues are already scaled here)

$$\phi_{(p_1^*)}^{[1]}(\zeta) = \frac{\zeta \cdot \overline{(z_\zeta)^{1/2}(p_1^*)} - \bar{\zeta} \cdot \overline{(\bar{z}_\zeta)^{1/2}(p_1^*)}}{|z_\zeta|(p_1^*) - |\bar{z}_\zeta|(p_1^*)} \frac{1}{(\zeta - p_1^*)} \\ \phi_{(p_1^*)}^{[i]}(\zeta) = \frac{\bar{\zeta} \cdot \overline{(z_\zeta)^{1/2}(p_1^*)} + \zeta \cdot \overline{(\bar{z}_\zeta)^{1/2}(p_1^*)}}{|z_\zeta|(p_1^*) - |\bar{z}_\zeta|(p_1^*)} \frac{1}{(\zeta - p_1^*)} = -i \phi_{(p_1^*)}^{[1]}(\zeta)$$

Recalling the relation (2.34), this gives that for $\mathfrak{p} \in \{1, i\}$

$$f_{(p_1^*)}^{[\mathfrak{p}]}(\zeta) = \frac{\bar{\zeta}(z_\zeta)^{\frac{1}{2}} \phi_{(p_1^*)}^{[\mathfrak{p}]}(\zeta) + \zeta(\bar{z}_\zeta)^{\frac{1}{2}} \overline{\phi_{(p_1^*)}^{[\mathfrak{p}]}(\zeta)}}{|z_\zeta| - |\bar{z}_\zeta|} \quad (4.5)$$

Finally, this simplifies as (using the end of Section 2.6 and [12, Section 2.7])

$$\begin{aligned} |F_\vartheta^*(p_1^*, p_2^*)|^2 - |F_\vartheta(p_1^*, p_2^*)|^2 &= 4 \operatorname{Re} [i \cdot f_{(p_1^*)}^{[1]}(p_2^*) \cdot \overline{f_{(p_1^*)}^{[i]}(p_2^*)}] \\ &= \frac{4}{l(p_1^*)l(p_2^*)} \frac{1}{|p_2^* - p_1^*|^2}, \end{aligned}$$

where $l(\zeta) = |z_\zeta| - |\bar{z}_\zeta|$ is the metric element at ζ and the distance $|p_2^* - p_1^*|$ is computed in the conformal coordinates. All together, this gives that

$$\frac{\cos(\theta_{e_1^\delta}) \cdot \cos(\theta_{e_2^\delta})}{r_{e_1^\delta} \cdot r_{e_2^\delta}} \cdot \mathbb{E}_{S^\delta}[\tilde{\varepsilon}_1 \cdot \tilde{\varepsilon}_2] = \frac{1}{\pi^2} \frac{1}{l(p_1^*)l(p_2^*)} \frac{1}{|p_2^* - p_1^*|^2} + o_{\delta \rightarrow 0}(1). \quad (4.6)$$

In particular, one recovers the classical result on the critical planar Ising model, but with this time with an additional composition coming from the conformal change of metric of the maximal surface. \square

Let us now turn to the proofs concerning bounded domains, beginning with doubly-periodic graphs (the argument extends straightforwardly to grids satisfying UNIF(δ) and FLAT(δ)), and then proceeding to maximal surfaces $(z, \vartheta(z)) \in \mathbb{R}^{(2,1)}$ arising from s -embeddings that satisfy UNIF(δ) and for which $|\mathcal{Q}^\delta - \vartheta| = O(\delta)$. In the latter setting, the hyperbolic metric element that appears is the one associated with the conformal parametrisation of $(z, \vartheta(z))$.

Proof of Theorem 1.4. Fix a corner a^δ belonging to $z^\delta \in \diamondsuit(G)$, attached to the edge e^δ , and assume that a^δ approximates an interior point $a \in \Omega$. We identify the corner a^δ with $v^\bullet(a^\delta)$ and with the vertex $v_+^\circ \in G^\circ$ carrying the spin $\sigma_{e_+^\delta}$. Suppose that $\operatorname{dist}(a^\delta, \partial\Omega) = 2r_0 > 0$. Using the correspondence (2.15), define $F_{\Omega^\delta}^{(a^\delta)}$ as the s -holomorphic function associated with $\delta_a^{-\frac{1}{2}} \langle \chi_c \chi_{a^\delta} \rangle_{\Omega^\delta}^{(w)}$, and $F_{S^\delta}^{(a^\delta)}$ as the s -holomorphic function corresponding to $\delta_a^{-\frac{1}{2}} \langle \chi_c \chi_{a^\delta} \rangle_{S^\delta}$. Finally, set

$$X^\delta(c) := \delta_a^{-\frac{1}{2}} (\langle \chi_c \chi_{a^\delta} \rangle_{\Omega^\delta}^{(w)} - \langle \chi_c \chi_{a^\delta} \rangle_{S^\delta}),$$

and denote by F_δ^\dagger the s -holomorphic function associated with X^δ . It is straightforward to verify that F_δ^\dagger remains s -holomorphic even at a^δ , since the singularities of $\langle \chi_c \chi_{a^\delta} \rangle_{\Omega^\delta}^{(w)}$ and $\langle \chi_c \chi_{a^\delta} \rangle_{S^\delta}$ exactly cancel each other. The first step is to establish the pre-compactness of the family $(F_{\Omega^\delta}^{(a^\delta)})_{\delta > 0}$.

Applying the integration procedure (2.19), let H_δ denote the primitive associated with $F_{\Omega^\delta}^{(a^\delta)}$ and H_δ^\dagger the one associated with F_δ^\dagger . For $r > 0$, set

$$M_r^\delta := \left(\max_{v \in \Omega^\delta \setminus D(a^\delta, r)} |H_\delta| \right)^{1/2}.$$

After passing to a subsequence, we may assume that $\eta_{a^\delta} \rightarrow \eta \in \mathbb{T}$. There are two possible scenarios, though the second will turn out to be impossible.

Scenario 1: The family $(M_{r_0}^\delta)_{\delta>0}$ is uniformly bounded. We claim that, in this case, one can extract a subsequential limit from the family $(F_{\Omega^\delta}^{(a^\delta)})_{\delta>0}$ away from the point a . The argument proceeds in two steps.

First, outside the disk $D(a^\delta, r_0)$, Theorem 2.1 and Remark 2.10 imply that $(F_{\Omega^\delta}^{(a^\delta)})_{\delta>0}$ is pre-compact. Moreover, since

$$F_\delta^\dagger = F_{\Omega^\delta}^{(a^\delta)} - F_{S^\delta}^{(a^\delta)}$$

is s -holomorphic *everywhere* in the bulk of Ω^δ (including at a^δ), the discrete maximum principle ensures that $|F_\delta^\dagger|$ remains bounded near a . Fix a discrete circle approximating the boundary of $D(a^\delta, r_0)$. As $\delta \rightarrow 0$, $|F_\delta^\dagger|$ remains uniformly bounded within $D(a^\delta, r_0)$. Since the functions $(F_{S^\delta}^{(a^\delta)})_{\delta>0}$ are uniformly bounded on compact subsets of $\mathbb{C} \setminus \{a\}$, it follows that the family $(F_{\Omega^\delta}^{(a^\delta)})_{\delta>0}$ is bounded and thus pre-compact on compact subsets of $\Omega \setminus \{a\}$.

Let f denote a subsequential limit of $(F_{\Omega^\delta}^{(a^\delta)})_{\delta>0}$. Since $F_{S^\delta}^{(a^\delta)} \rightarrow \overline{\eta_a} \pi^{-1}(z-a)^{-1}$ uniformly on compact subsets of $\mathbb{C} \setminus \{a\}$, one has

$$H_\delta \rightarrow h := \operatorname{Im} \left[\int f^2 dz \right] \quad \text{and} \quad H_\delta^\dagger \rightarrow h^\dagger := \operatorname{Im} \left[\int (f - \overline{\eta_a} \pi^{-1}(z-a)^{-1})^2 dz \right],$$

where f satisfies the following properties:

- (1) f is holomorphic and h is harmonic in $\Omega \setminus \{a\}$.
- (2) $f - \frac{\overline{\eta_a}}{\pi(z-a)}$ is uniformly bounded near a .
- (3) h vanishes identically on $\partial\Omega$.
- (4) For any $v \in \partial\Omega$, one has $\partial_{(i\tau_v)} h \geq 0$, where τ_v denotes the unit tangent vector to $\partial\Omega$ at v , oriented so that Ω lies to its left.

The first item follows directly from Theorem 2.1 and Remark 2.10. To establish the second, note that the discrete maximum principle applied to F_δ^\dagger guarantees that $f - \overline{\eta_a} \pi^{-1}(z-a)^{-1}$ remains uniformly bounded near a , and hence extends holomorphically through a .

We now address the third item, namely the persistence of Dirichlet boundary conditions for H_δ in the continuous limit. Recall that H_δ satisfies zero boundary conditions along $\partial\Omega^\delta$, due to the wired boundary conditions. Consider a small boundary arc $\ell \subset \partial\Omega$, discretized by $\ell_\delta \subset \partial\Omega^\delta$, connecting two prime ends m and n (approximated by m^δ and n^δ). Let ℓ' be another nontrivial arc inside Ω connecting m and n while staying at distance r_0 from a , and let $\widehat{\Omega}$ denote the domain enclosed by $\ell \cup \ell'$. Assume that $\widehat{\Omega}^\delta \subset \Omega^\delta$ is the discrete domain bounded by the wired arc ℓ^δ and the free arc ℓ'_δ , approximating ℓ' . The function H^δ is bounded on $\widehat{\Omega}^\delta$, and by [12, Theorem 4.1], the functions H^δ and their continuous harmonic extensions on $\widehat{\Omega}^\delta$ are polynomially close within a $\delta^{1-\eta}$ -interior of $\widehat{\Omega}^\delta$. It follows (as in [12, Proof of Theorem 1.2]) that the discrete Dirichlet boundary conditions for H^δ persist in the limit, implying that h vanishes along ℓ . Varying ℓ along $\partial\Omega$ proves the third item.

Finally, for the last item, let $F_{\widehat{\Omega}^\delta}$ denote the FK observable with *wired* boundary conditions on ℓ_δ° and *free* boundary conditions on ℓ'_δ^\bullet , as defined in [12, Section 2.4]. Set $\widehat{H}^\delta = H[F_{\widehat{\Omega}^\delta}]$ and $G^\delta = H[F^\delta, F_{\widehat{\Omega}^\delta}]$ via (2.19). As in the case of H^δ , the

boundary conditions for both \hat{H}^δ and G^δ persist in the continuous limit. Consequently, $F_{\hat{\Omega}^\delta}$ converges to f_{FK} , the limiting FK observable in the domain $\hat{\Omega}$. Since Ω is smooth, both f and f_{FK} extend continuously up to the boundary, and $G^\delta \rightarrow g = \int \text{Im}[f \cdot f_{\text{FK}} dz]$. For $v \in l$, the vanishing of g along l , combined with the estimate $f_{\text{FK}} \in \sqrt{\tau_v}$, implies that $f \in \sqrt{\tau_v}$, hence $\partial_{(i\tau_v)} h \geq 0$.

Scenario 2: $(M_{r_0}^\delta)_{\delta>0}$ diverges to infinity along some subsequence. We keep the notations of the previous paragraph, setting

$$\tilde{F}_{\Omega^\delta}^{(a^\delta)} := (M_{r_0}^\delta)^{-1} F_{\Omega^\delta}^{(a^\delta)}, \quad \tilde{F}_\delta^\dagger := (M_{r_0}^\delta)^{-1} F_\delta^\dagger, \quad \tilde{H}_\delta := (M_{r_0}^\delta)^{-2} H_\delta, \quad \tilde{H}_\delta^\dagger := (M_{r_0}^\delta)^{-2} H_\delta^\dagger.$$

In this case, one can repeat the reasoning of Scenario 1 for the family $(\tilde{F}_{\Omega^\delta}^{(a^\delta)})_{\delta>0}$, which converges uniformly on compact subsets of $\Omega \setminus \{a\}$ to some limit \tilde{f} . Without loss of generality (up to extracting another subsequence), we may also assume the existence of points $v^\delta \rightarrow v_\infty \in \Omega \setminus D(a, \frac{1}{2}r_0)$ such that $|\tilde{H}_\delta(v^\delta)| = 1$.

By the discrete maximum principle for s -holomorphic functions, together with the observation that $(M_{r_0}^\delta)^{-1} F_{S^\delta}^{(a^\delta)} \rightarrow 0$ uniformly on compact subsets of $\Omega \setminus \{a\}$, we obtain $\tilde{F}_\delta^\dagger \rightarrow \tilde{f}^\dagger = \tilde{f}$. Consequently, \tilde{f} is holomorphic in $\Omega \setminus \{a\}$ and bounded near a , hence extends holomorphically through a . Uniformly on compact subsets of Ω , we then have $\tilde{H}_\delta \rightarrow \tilde{h} := \text{Im}[\int \tilde{f}^2 dz]$, which inherits the zero Dirichlet boundary conditions of \tilde{H}_δ along $\partial\Omega$ in the limit. In particular, \tilde{h} is harmonic throughout Ω , vanishes identically on $\partial\Omega$, and thus must vanish everywhere in Ω . This contradicts the normalization $|\tilde{h}(v_\infty)| = 1$, showing that this second scenario cannot occur.

The conclusion of the above dichotomy is that $F_{\Omega^\delta}^{(a^\delta)}$ converges to a unique function $f^{[\eta_a]}$ satisfying the four properties listed above. As shown in [16, Definition 3.12], such a function exists and is unique. Moreover, $f^{[\eta_a]}$ admits the following decomposition (see, for instance, [16, Lemma 3.17]):

$$f^{[\eta_a]}(z) = \frac{1}{2}(\overline{\eta_a} f_\Omega(a, z) + \eta_a f_\Omega^*(a, z)), \quad (4.7)$$

where $f_\Omega(a, z)$ is holomorphic in both variables, $f_\Omega^*(a, z)$ is holomorphic in z and anti-holomorphic in a , and they satisfy $f_\Omega(a, z) = -f_\Omega(z, a)$ and $f_\Omega^*(a, z) = -\overline{f_\Omega^*(z, a)}$. When $\Omega = \mathbb{H}$, one has $f_\Omega(a, z) = 2[\pi(z - a)]^{-1}$ and $f_\Omega^*(a, z) = 2[\pi(z - \bar{a})]^{-1}$.

Given a conformal map $\varphi : \Omega \rightarrow \Omega'$, these functions transform as

$$f_\Omega(a, z) = f_{\Omega'}(\varphi(a), \varphi(z))(\varphi'(a)\varphi'(z))^{1/2}, \quad f_\Omega^*(a, z) = f_{\Omega'}^*(\varphi(a), \varphi(z))(\overline{\varphi'(a)}\varphi'(z))^{1/2}.$$

Using the explicit expressions in \mathbb{H} , one obtains for any domain that $f_\Omega(a, z) = 2[\pi(z - a)]^{-1} + o_{z \rightarrow a}(1)$, while $f_\Omega^*(a, z) = -i\pi^{-1}\ell_\Omega(a) + o_{z \rightarrow a}(1)$. Altogether, this yields the expansion

$$f^{[\eta_a]}(z) = \frac{\overline{\eta_a}}{\pi(z - a)} - \frac{i\eta_a \ell_\Omega(a)}{\pi} + o_{z \rightarrow a}(1). \quad (4.8)$$

We are now in position to conclude. Recall that the corner b^δ is the neighbor of a^δ in z_{e^δ} and shares the same primal vertex. It follows immediately that $X^\delta(a^\delta) = 0$ and

$$X^\delta(b^\delta) = \delta_a^{-\frac{1}{2}} (\mathbb{E}_{\Omega^\delta}^{(w)}[\varepsilon_{e^\delta}] - \mathbb{E}_{S^\delta}^{(w)}[\varepsilon_{e^\delta}]).$$

Using (2.15), we obtain

$$F_\delta^\dagger(z_{e^\delta}) = -i\eta_a \frac{\mathbb{E}_{\Omega^\delta}^{(w)}[\varepsilon_{e^\delta}] - \mathbb{E}_{\mathcal{S}^\delta}^{(w)}[\varepsilon_{e^\delta}]}{(\delta_a \delta_b)^{1/2} \sin(\phi_{v^\bullet(a^\delta)} z_{e^\delta})}. \quad (4.9)$$

Applying the discrete maximum principle to F_δ^\dagger , together with the fact that $f^{[\eta_a]}(z) - \frac{\eta_a}{\pi(z-a)}$ extends holomorphically through a , yields

$$\lim_{\delta \rightarrow 0} \frac{\mathbb{E}_{\Omega^\delta}^{(w)}[\varepsilon_{e^\delta}] - \mathbb{E}_{\mathcal{S}^\delta}^{(w)}[\varepsilon_{e^\delta}]}{(\delta_a \delta_b)^{1/2} \sin(\phi_{v^\bullet(a^\delta)} z_{e^\delta})} = \frac{\ell_\Omega(a)}{\pi}. \quad (4.10)$$

The identities in (2.9) then allow us to conclude the proof. \square

Let us now pass to the proof of Theorem 1.5, which ressembles the proof of Theorem 1.4, with an additional complication coming from the change of metric in the conformal parametrisation of the maximal surface $(z, \vartheta(z)) \in \mathbb{R}^{2,1}$.

Proof of Theorem 1.5. Recall that in this special case of maximal surfaces, the parametrisation (2.31) $\zeta \mapsto z(\zeta)$ of the surface $(z, \vartheta(z))$ is both conformal and harmonic. We now consider the full-plane parametrisation, and denote by Ω^* the pre-image of Ω . We keep the notations from the previous proof.

In fact, one easily observes that it suffices to treat the first scenario from the preceding analysis: the convergence of the FK observables [51] rules out, by the same argument as in the periodic case, the possibility of the second scenario. We therefore assume once again that we are in Scenario 1, so that the functions $(F_{\Omega^\delta}^{(a^\delta)})_{\delta > 0}$ remain bounded and hence pre-compact on compact subsets of $\Omega \setminus \{a\}$. Let f_Ω be a subsequential limit of $(F_{\Omega^\delta}^{(a^\delta)})_{\delta > 0}$ and $f_{\mathbb{C}}$ a subsequential limit of $(F_{\mathcal{S}^\delta}^{(a^\delta)})_{\delta > 0}$, assuming (after passing to a further subsequence if necessary) that $\eta_{a^\delta} \rightarrow \eta_a \in \mathbb{T}$. We again perform the change of variables (2.34), defining in the ζ parametrisation

$$\begin{aligned} \phi_\Omega(\zeta) &:= \bar{\zeta} f_\Omega(z(\zeta))(z_\zeta)^{1/2} + \zeta \overline{f_\Omega(z(\zeta))} (\bar{z}_\zeta)^{1/2}, \\ \phi_{\mathbb{C}}(\zeta) &:= \bar{\zeta} f_{\mathbb{C}}(z(\zeta))(z_\zeta)^{1/2} + \zeta \overline{f_{\mathbb{C}}(z(\zeta))} (\bar{z}_\zeta)^{1/2}. \end{aligned}$$

In this setting, one can deduce directly from [18, Proposition 2.21] that, uniformly on compact subsets of $\Omega \setminus \{a\}$ (respectively $\Omega^* \setminus \{a^*\}$), the functions $H^\delta = H[F_{\Omega^\delta}^{(a^\delta)}]$ converge to

$$h = \int \text{Im}[f_\Omega^2 dz] + |f_\Omega|^2 d\vartheta = \int \text{Im}[\phi_\Omega^2 d\zeta]. \quad (4.11)$$

Both ϕ_Ω and $\phi_{\mathbb{C}}$ are holomorphic away from a . The function ϕ_Ω satisfies the following properties:

- (1) ϕ_Ω is holomorphic in $\Omega^* \setminus \{a^*\}$, as a consequence of [18, Proposition 2.21] (and the same holds for $\phi_{\mathbb{C}}$);
- (2) $\phi_\Omega - \phi_{\mathbb{C}}$ remains uniformly bounded near a ;
- (3) h is harmonic in $\Omega^* \setminus \{a^*\}$ and vanishes identically on $\partial\Omega^*$;
- (4) for any $v^* \in \partial\Omega$, one has $\partial_{(i\tau_{v^*})} h \geq 0$, where τ_{v^*} denotes the unit tangent vector to $\partial\Omega$ at v^* , oriented so that Ω^* lies on its left.

The second property follows from the fact that F_δ^\dagger satisfies the discrete maximum principle near a^δ , ensuring that convergence in the bulk implies uniform boundedness near a . The third and fourth items follow exactly as in the previous theorem, this time using the analogue of [12, Theorem 4.1] for maximal surfaces $(z, \vartheta(z))$.

We now derive the explicit expression of $\phi_{\mathbb{C}}$ as a simple meromorphic function with a single pole at a^* . Following the proof of [18, Proposition 3.6], $\phi_{\mathbb{C}}$ can have at most one simple pole near a^* , due to the one-sided boundedness of the projection of $\int(\bar{\zeta}f_{\mathbb{C}} dz + \zeta\bar{f}_{\mathbb{C}} d\vartheta)$. Since the monodromy of $g_{\mathbb{C}}$ around a is $2i\bar{\eta}_a$, one can use relation (2.38) in the ζ -parametrisation and reproduce the argument of [18, Proof of Proposition 3.6] to obtain

$$\phi_{\mathbb{C}}(\zeta) = \frac{1}{\pi} \overline{\mu^*} \frac{1}{\zeta - a^*} + O_{\zeta \rightarrow a}(1), \quad (4.12)$$

where the coefficient μ^* is given by

$$\mu^* = \frac{\bar{\varsigma} \eta_a (z_{\zeta})^{1/2}(a^*) - \varsigma \bar{\eta}_a (\bar{z}_{\zeta})^{1/2}(a^*)}{|z_{\zeta}|(a^*) - |\bar{z}_{\zeta}|(a^*)}. \quad (4.13)$$

To verify this correspondence, one must align the notations used in [18, Proposition 3.6] with those of the present work. The coefficient μ and the function $\psi_{\mathfrak{w}}$ in [18, Proposition 3.6] correspond respectively to μ^* and $\phi_{\mathbb{C}}$ here. Furthermore, the prefactor in the origami square root differs: $\varsigma = 1$ in [18], whereas $\varsigma = e^{i\frac{\pi}{4}}$ here. This change modifies the prefactors of the η -terms in μ^* compared to μ , and transforms the prefactor of $\psi^{[+,+]}$ from $\frac{1}{i\pi}$ in [18] to $\frac{1}{\pi}$ in the current setting.

Moreover, $h_{\mathbb{C}} = \int \text{Im}[\phi_{\mathbb{C}}(\zeta)^2 d\zeta]$ is harmonic (again by [18, Proposition 3.6]) except at a^* , and is bounded at infinity-this follows from the decay $f_{\mathbb{C}}(z) = O(|z - a|^{-1})$ and the fact that the full plane parametrisation (2.31) is proper. Hence all non-negative coefficients in the Laurent expansion of $\phi_{\mathbb{C}}$ around a^* vanish, yielding

$$\phi_{\mathbb{C}}(\zeta) = \frac{1}{\pi} \overline{\mu^*} \frac{1}{\zeta - a^*}. \quad (4.14)$$

We are now ready to conclude. Recall that F_{δ}^{\dagger} is s -holomorphic in a macroscopic neighbourhood of the corner a , and that $F_{\delta}^{\dagger}(z_e) \in i\eta_{a^*}\mathbb{R}$. It follows that there exists $l_a \in \mathbb{R}$ such that, uniformly in a fixed neighbourhood of a , one has

$$F_{\delta}^{\dagger}(z) = i\eta_a l_a + o_{\delta \rightarrow 0}(1) + o_{z \rightarrow a}(1).$$

Repeating the argument used in the proof of Theorem 1.4, but replacing $f^{[\eta]}$ by ϕ_{Ω} , shows that l_a satisfies

$$\bar{\varsigma} i \eta_a l_a (z_{\zeta})^{1/2}(a^*) - \varsigma i \bar{\eta}_a l_a (\bar{z}_{\zeta})^{1/2}(a^*) = -i \frac{\mu^* \ell_{\Omega^*}(a^*)}{\pi}. \quad (4.15)$$

Using the explicit expression of μ^* and the reasoning at the end of the proof of Theorem 1.4, we finally obtain

$$\lim_{\delta \rightarrow 0} \cos(\theta_{e^{\delta}}) \frac{\mathbb{E}_{\Omega^{\delta}}^{(w)}[\varepsilon_{e^{\delta}}] - \mathbb{E}_{\mathcal{S}^{\delta}}[\varepsilon_{e^{\delta}}]}{r_{z_{e^{\delta}}}} = \frac{\ell_{\Omega^*}(a^*)}{\pi(|z_{\zeta}|(a^*) - |\bar{z}_{\zeta}|(a^*))}. \quad (4.16)$$

□

REFERENCES

[1] Sung Chul, Tuomas Vitarnen, and Christian Webb. “Near-critical Ising, sine-Gordon at the free fermion point, and bosonization”. In: *arXiv preprint 2512.11304* (2025).

- [2] Niklas Christoph Affolter et al. “Discrete Lorentz surfaces and s-embeddings I: isothermic surfaces”. In: *Journal of Geometry and Physics* 213 (2025), p. 105482.
- [3] Niklas Christoph Affolter et al. “Discrete Lorentz surfaces and s-embeddings II: maximal surfaces”. In: *arXiv preprint arXiv:2411.19055* (2024).
- [4] Michael Aizenman et al. “Emergent planarity in two-dimensional Ising models with finite-range interactions”. In: *Inventiones mathematicae* 216 (2019), pp. 661–743.
- [5] *Elliptic Partial Differential Equations and Quasiconformal Mappings in the Plane (PMS-48)*. Princeton University Press, 2008.
- [6] Mikhail Basok. *Dimers on Riemann surfaces and compactified free field*. arXiv preprint 2309.14522. 2023. URL: <https://arxiv.org/abs/2309.14522>.
- [7] Alexander A Belavin, Alexander M Polyakov, and Alexander B Zamolodchikov. “Infinite conformal symmetry of critical fluctuations in two dimensions”. In: *Journal of Statistical Physics* 34 (1984), pp. 763–774.
- [8] Nathanaël Berestycki, Benoit Laslier, and Gourab Ray. “A note on dimers and T-graphs”. In: *arXiv preprint arXiv:1610.07994* (2016).
- [9] Ahmed Bou-Rabee and Ewain Gwynne. “Random walk on sphere packings and Delaunay triangulations in arbitrary dimension”. In: *arXiv preprint arXiv:2405.11673* (2024).
- [10] Cédric Boutillier, Béatrice de Tilière, and Kilian Raschel. “The Z-invariant massive Laplacian on isoradial graphs”. In: *Inventiones mathematicae* 208.1 (2017), pp. 109–189.
- [11] Cédric Boutillier, Béatrice de Tilière, and Kilian Raschel. “The Z-invariant Ising model via dimers”. In: *Probability Theory and Related Fields* 174.1 (2019), pp. 235–305.
- [12] Dmitry Chelkak. “Ising model and s-embeddings of planar graphs”. English. In: *Ann. Sci. Éc. Norm. Supér. (4)* 57.5 (2024), pp. 1271–1346. ISSN: 0012-9593. DOI: 10.24033/asens.2591.
- [13] *Planar Ising model at criticality: state-of-the-art and perspectives*. World Sci. Publ., Hackensack, NJ, 2018, pp. 2801–2828.
- [14] Dmitry Chelkak, David Cimasoni, and Adrien Kassel. “Revisiting the combinatorics of the 2D Ising model”. In: *Annales de l’Institut Henri Poincaré D* 4.3 (2017), pp. 309–385.
- [15] Dmitry Chelkak, Clément Hongler, and Konstantin Izyurov. “Conformal invariance of spin correlations in the planar Ising model”. In: *Ann. of Math. (2)* 181.3 (2015), pp. 1087–1138. ISSN: 0003-486X. DOI: 10.4007/annals.2015.181.3.5. URL: <http://dx.doi.org/10.4007/annals.2015.181.3.5>.
- [16] Dmitry Chelkak, Clément Hongler, and Konstantin Izyurov. “Correlations of primary fields in the critical Ising model”. In: *arXiv preprint arXiv:2103.10263* (2021).
- [17] Dmitry Chelkak, Konstantin Izyurov, and Rémy Mahfouf. “Universality of spin correlations in the Ising model on isoradial graphs”. In: *The Annals of Probability* 51.3 (2023), pp. 840–898.
- [18] Dmitry Chelkak, Benoît Laslier, and Marianna Russkikh. “Bipartite dimer model: perfect t-embeddings and Lorentz-minimal surfaces”. In: *arXiv preprint 2109.06272* (2021).

- [19] Dmitry Chelkak, Benoît Laslier, and Marianna Russkikh. “Dimer model and holomorphic functions on t-embeddings of planar graphs”. English. In: *Proc. Lond. Math. Soc. (3)* 126.5 (2023), pp. 1656–1739. ISSN: 0024-6115. DOI: 10.1112/plms.12516.
- [20] Dmitry Chelkak and Stanislav Smirnov. “Universality in the 2D Ising model and conformal invariance of fermionic observables”. In: *Invent. Math.* 189.3 (2012), pp. 515–580. ISSN: 0020-9910. DOI: 10.1007/s00222-011-0371-2. URL: <http://dx.doi.org/10.1007/s00222-011-0371-2>.
- [21] David Cimasoni and Hugo Duminil-Copin. “The critical temperature for the Ising model on planar doubly periodic graphs”. In: *Electron. J. Probab.* 18 (2013), no. 44, 18. ISSN: 1083-6489. DOI: 10.1214/EJP.v18-2352. URL: <https://doi.org/10.1214/EJP.v18-2352>.
- [22] Viktor S Dotsenko and Vladimir S Dotsenko. “Critical behaviour of the phase transition in the 2D Ising model with impurities”. In: *Advances in Physics* 32.2 (1983), pp. 129–172.
- [23] Julien Dubédat. “Dimers and families of Cauchy-Riemann operators I”. In: *Journal of the American Mathematical Society* 28.4 (2015), pp. 1063–1167.
- [24] Julien Dubédat. “Exact bosonization of the Ising model”. In: *arXiv preprint 1112.4399* (2011).
- [25] Hugo Duminil-Copin. “Parafermionic observables and their applications to planar statistical physics models”. In: *Ensaio Matemático* 25 (2013), pp. 1–371.
- [26] Hugo Duminil-Copin, Clément Hongler, and Pierre Nolin. “Connection probabilities and RSW-type bounds for the two-dimensional FK Ising model”. In: *Communications on pure and applied mathematics* 64.9 (2011), pp. 1165–1198.
- [27] S. Friedli and Y. Velenik. *Statistical mechanics of lattice systems*. A concrete mathematical introduction. Cambridge University Press, Cambridge, 2018, pp. xix+622. ISBN: 978-1-107-18482-4.
- [28] Reza Gheissari, Clément Hongler, and SC Park. “Ising model: local spin correlations and conformal invariance”. In: *Communications in Mathematical Physics* 367 (2019), pp. 771–833.
- [29] Ori Gurel-Gurevich, Daniel C Jerison, and Asaf Nachmias. “A combinatorial criterion for macroscopic circles in planar triangulations”. In: *arXiv preprint arXiv:1906.01612* (2019).
- [30] Clément Hongler. “Conformal invariance of Ising model correlations”. PhD thesis. University of Geneva, 2010.
- [31] Clément Hongler and Stanislav Smirnov. “The energy density in the planar Ising model”. In: *Acta Math.* 211.2 (2013), pp. 191–225. ISSN: 0001-5962. DOI: 10.1007/s11511-013-0102-1. URL: <http://dx.doi.org/10.1007/s11511-013-0102-1>.
- [32] Leo P. Kadanoff and Horacio Ceva. “Determination of an operator algebra for the two-dimensional Ising model”. In: *Phys. Rev. B (3)* 3 (1971), pp. 3918–3939. ISSN: 0163-1829.
- [33] Carlos Kenig et al. “A new approach to absolute continuity of elliptic measure, with applications to non-symmetric equations”. In: *Advances in mathematics* 153.2 (2000), pp. 231–298.

- [34] Carlos E Kenig and Wei-Ming Ni. “On the elliptic equation”. In: *Annali della Scuola Normale Superiore di Pisa-Classe di Scienze* 12.2 (1985), pp. 191–224.
- [35] Richard Kenyon. “The asymptotic determinant of the discrete Laplacian”. In: *Acta Math.* 185.2 (2000), pp. 239–286. ISSN: 0001-5962.
- [36] Richard Kenyon et al. “Dimers and circle patterns”. English. In: *Ann. Sci. Éc. Norm. Supér. (4)* 55.3 (2022), pp. 865–903. ISSN: 0012-9593. DOI: 10.24033/asens.2507.
- [37] Richard W Kenyon and Scott Sheffield. “Dimers, tilings and trees”. In: *Journal of Combinatorial Theory, Series B* 92.2 (2004), pp. 295–317.
- [38] Marcin Lis. “Circle patterns and critical Ising models”. In: *Communications in Mathematical Physics* 370.2 (2019), pp. 507–530.
- [39] Rémy Mahfouf. “Analyse du modèle d’Ising planaire au-delà du cadre critique Z-invariant”. PhD thesis. Université Paris-Saclay, 2022.
- [40] Rémy Mahfouf. “Crossing estimates for the Ising model on general s-embeddings”. In: *Proceedings of the London Mathematical Society* 131.4 (2025), e70092.
- [41] Rémy Mahfouf. “Conformal invariance of Ising spin correlation on critical doubly-periodic graphs”. In: *arXiv preprint* ().
- [42] Rémy Mahfouf. “The near-critical random bond Ising model via embedding deformation”. In: *arXiv preprint: 2509.08928* ().
- [43] Barry M McCoy, Craig A Tracy, and Tai Tsun Wu. “Painlevé functions of the third kind”. In: *Journal of Mathematical Physics* 18.5 (1977), pp. 1058–1092.
- [44] Barry M. McCoy and Tai Tsun Wu. *The two-dimensional Ising model*. Second. Corrected reprint of [MR3618829], with a new preface and a new chapter (Chapter XVII). Dover Publications, Inc., Mineola, NY, 2014, pp. xvi+454. ISBN: 978-0-486-49335-0; 0-486-49335-0.
- [45] Christian Mercat. “Discrete Riemann surfaces and the Ising model”. In: *Comm. Math. Phys.* 218.1 (2001), pp. 177–216. ISSN: 0010-3616. DOI: 10.1007/s002200000348. URL: <http://dx.doi.org/10.1007/s002200000348>.
- [46] Basok Mikhail et al. “Harmonic functions on Tutte’s embeddings and linearized Monge-Ampere equation”. In: *arXiv preprint 2511.06587* (2025).
- [47] Lars Onsager. “Crystal statistics. I. A two-dimensional model with an order-disorder transition”. In: *Physical review* 65.3-4 (1944), p. 117.
- [48] John Palmer. *Planar Ising Correlations*. Vol. 49. Springer Science & Business Media, 2007.
- [49] S. C. Park. “Massive Scaling Limit of the Ising Model: Subcritical Analysis and Isomonodromy”. In: (2018).
- [50] SC Park. “Convergence of fermionic observables in the massive planar FK-Ising model”. In: *Communications in mathematical physics* 396.3 (2022), pp. 1071–1133.
- [51] Sung Chul Park. “Conformal invariance of the FK-Ising model on Lorentz maximal s-embeddings”. In: *arXiv preprint 2512.10142* (2025).
- [52] Jacques HH Perk. “Quadratic identities for Ising model correlations”. In: *Physics Letters A* 79.1 (1980), pp. 3–5.
- [53] Mikio Sato, Tetsuji Miwa, and Michio Jimbo. “Holonomic quantum fields. IV”. In: *Publications of the Research Institute for Mathematical Sciences* 15.3 (1979), pp. 871–972.
- [54] Stanislav Smirnov. “Conformal invariance in random cluster models. I. Holomorphic fermions in the Ising model”. In: *Ann. of Math.* (2) 172.2 (2010),

pp. 1435–1467. ISSN: 0003-486X. DOI: 10.4007/annals.2010.172.1441.
URL: <https://doi.org/10.4007/annals.2010.172.1441>.

- [55] Stanislav Smirnov. “Towards conformal invariance of 2D lattice models”. In: *In International Congress of Mathematicians. Vol. II, pages 1421–1451. Eur. Math. Soc., Zürich* (2006).
- [56] Béatrice de Tilière. “The Z-Dirac and massive Laplacian operators in the Z-invariant Ising model”. In: *Electronic Journal of Probability* 26 (2021), pp. 1–86.
- [57] William Thomas Tutte. “How to draw a graph”. In: *Proceedings of the London Mathematical Society* 3.1 (1963), pp. 743–767.
- [58] Yijun Wan. “Statistical mechanics models via the lens of potential theory”. PhD thesis. Université Paris-Saclay, 2022.
- [59] AB Zamolodchikov. “Exact solutions of conformal field theory in two dimensions and critical phenomena”. In: *Reviews in Mathematical Physics* 1.02n03 (1989), pp. 197–234.